I. A STUDY OF VIBRATIONAL RELAXATION IN CARBON MONOXIDE BY SHOCK-WAVES AND INFRA-RED EMISSION

II. A STUDY OF THE EFFECT OF A RESONANT TRANSFER OF ENERGY ON THE VIBRATIONAL RELAXATION OF GAS MIXTURES

Thesis by

Raymond Leonard Taylor

In Partial Fulfillment of the Requirements

For the Degree of

Doctor of Philosophy

California Institute of Technology

Pasadena, California

1960

ACKNOWLEDGEMENT

I have been privileged to work under the direction of Dr. Norman Davidson here at the Institute. His guidance, enthusiasm, and friendship are deeply appreciated. It was also a pleasure to collaborate with Dr. Maurice W. Windsor on part of the research described in this thesis. I am appreciative of the many members of the faculty and students of the Institute who have given me advice, criticism, and friendship during these years.

The research described in this thesis was supported by the Office of Naval Research. Financial assistance was obtained from the Institute in the form of teaching assistantships, tuition grants, and summer support. The duPont Company also contributed a teaching fellowship.

ABSTRACT

I. Pure CO gas was rapidly heated by the passage of a shock wave, and the vibrational relaxation time determined from measurements of the time history of the intensity of the 1st overtone transition at 2.35 μ. The relaxation time was measured over a temperature range of 1400 - 3000°K and at pressures from $1\frac{1}{2}$ - 4 atmospheres. At 1400°K and 1 atm. a value of 650 ± 50 μsec. was obtained. A large impurity effect was discovered and is believed to be caused by traces of water vapor.

II. The effect of an efficient, near-resonant exchange of vibrational energy between O_2 and N_2 molecules on the vibrational relaxation behavior was investigated. The near-resonant and non-resonant vibrational transition probabilities were estimated from current theory. It was shown that the resonant process can provide a catalytic path for the rapid vibrational relaxation of the slower component (N_2). The hypothetical calculations are compared with experiment, and an interpretation of the "impurity effect" of H_2O is given in terms of a resonant process.

TABLE OF CONTENTS

PAGE

II. A STUDY OF THE EFFECT OF A RESONANT TRANSFER OF ENERGY ON THE VIBRATIONAL RELAXATION OF GAS MIXTURES

I. A STUDY OF VIBRATIONAL RELAXATION IN CARBON MONOXIDE BY SHOCK-WAVE AND INFRA-RED EMISSION*

by M. Windsor, N. Davidson, and R. Taylor

Introduction

The interchange of energy between external degrees of freedom (translation) and the internal degrees of freedom (vibration and rotation) of a molecule when it undergoes a collision, is a subject of great importance, because of its intrinsic interest, because of its significance in the general field of chemical kinetics, and because of its bearing on various gas dynamical and combustion problems. When a gas is suddenly heated, as for example, by a shock-wave, or suddenly cooled, as by a rapid expansion, it undergoes a rapid change in temperature. In our normal usage of the term "temperature" we mean that the kinetic energy of translation of the molecules has changed. If the change is very sudden, the new distribution of molecular velocities may instantaneously even no longer follow the Maxwell-Boltzmann law. A new Boltzmann distribution is established in the time of a few collisions. To achieve complete thermodynamic equilibrium, it is now necessary for the energies of the rotational and the vibrational degrees of freedom to become adjusted. This will involve a further change of temperature as interchange of energy between translation and rotation and vibration takes place. The collisional processes by which this equilibration is effected are called rotational and vibrational relaxation.

Rotational relaxation usually takes only a few to a few tens of collisions, corresponding to a time of about 10^{-9} sec at STP. Rotation and

---

* To be published in the forthcoming book: "Proceedings of the Seventh International Symposium on Combustion," Butterworths Scientific Publications, London.

translation may, for most purposes therefore, be grouped together as external degrees of freedom. The transfer of energy between vibrations and external degrees of freedom, on the other hand, often turns out to be a very inefficient process. This is especially so for simple stiff diatomic molecules such as nitrogen, where many hundreds of thousands or even millions of collisions may be required. The relaxation time is long enough to make the question of vibrational relaxation assume practical importance. It affects, for example, the state of a gas undergoing rapid expansion in a rocket nozzle or suffering rapid compression behind a shock-wave.

With increasing molecular complexity, vibrational relaxation is more rapid, less than 90 collisions being required for propane at 20°C and 1 atm. It is still not uncommon, however, to find several thousand collisions necessary and in special cases, as in CO_2 at room temperature, the relaxation time may still be as long as several microseconds.

These statements apply to the pure gas. The study of molecules with long relaxation times is almost always complicated by the fact that polyatomic molecules usually make much more efficient collision partners for relaxation than another molecule of the pure gas. Minute amounts of polyatomic impurities may therefore reduce the observed times by several orders of magnitude. The commonest contaminant is water vapor and the problem of its removal will be discussed later on.

A number of methods have been employed for measuring relaxation times. These include: (1) the dispersion and absorption of ultrasonic waves,[1] (2) the impact tube,[1] (3) interferometric measurements of density changes behind shock-waves,[1,2] (4) a direct method involving infra-red radiation, called the spectrophone technique,[3] (5) the infra-red emission method described here.

In the present work a new technique for measuring vibrational relaxation times has been developed.[4] The rate of population of a particular vibrationally excited state in a gas that has been rapidly heated by the passage of a shock-wave is followed by observing the emission of infra-red radiation from this state with a detector of short response time.

In the particular application described here, we observe the rate of population of the 2 d vibrational state ($v = 2$) of CO from the time dependence of the emission of the first overtone ($2 \rightarrow 0$) radiation at 2.335 μ. (To some extent, of course, one is also looking at the transitions, $3 \rightarrow 1$, $4 \rightarrow 2$, etc., and hence at the population of these upper states.) The radiative lifetime for the $2 \rightarrow 0$ transition is 1.1 sec.[5] At equilibrium at 1 atm at 1500°K the calculated emission is 7.2×10^{-3} watts cc^{-1}, which, in the experimental arrangement, is readily detected. It is difficult to calculate self-absorption accurately, but approximate calculations according to the method of Penner and Weber[6] indicate that it is small or negligible (Actually, the amount of radiation is proportional to the population of the $v = 2$ state even if there is self-absorption provided that the amount of self-absorption is fairly constant; and specifically if it is not large in the boundary layer where the density and temperature are quite different than that of the bulk gas.) The lifetime for the $2 \rightarrow 1$ transition is 0.015 sec[5]; in our experiments, the lifetime for the $2 \rightarrow 0$ overall transition by collision is 10^{-3} sec or less. Therefore, the radiative processes serve to indicate the population of the state without significantly affecting it.

Experimental

The Shock Tube. The use of the shock tube in this laboratory as a tool for studying chemical reactions at high temperatures has already been described.[7] In all of our previous work the progress of a chemical reaction has been followed by the absorption of visible or ultraviolet light.

The length of our shock tube has been increased in order to improve the quality of the shocks and to increase the time available for observations. The diameter is 15 cm; the driving section is a 270 cm length of aluminum pipe; the shock wave section consists of a 140 cm length of aluminum pipe and two 150 cm lengths of pyrex pipe.

Part of the motivation to lengthen the tube was the desire to make observations in the region behind the reflected shock front which would have previously been terminated far too soon by the arrival of disturbances from the driving section. Reflected shock studies have several advantages. In the first place, the gas behind the reflected shock is stationary, so that the time-compression effect associated with the fact that the gas behind the incident shock is moving, does not occur. The removal of this penalty was important since our detector was already a limiting factor and we could ill afford to sacrifice any of its limited response time. Secondly, almost a millisecond was available before the arrival of the cold front. Finally, due to the double compression and heating, high temperatures and pressures could be reached without excessively high driving pressures and using less carbon monoxide. All of the experimental results presented here were made using the reflected shock technique. The observation station was set up as close as possible to the end-plate to minimize disturbances due to the growth of the boundary layer and to get the maximum observation time. The distance

chosen was 3 cm. With the optical system employed, this was enough to prevent the detector seeing possible radiation from the end-plate.

The Infra-red Cell. A lead sulfide photoconductive detector made by The Electronics Corporation of America was used. The sensitive element was 3 mm by 3 mm. The response time was 12 ± 3 μsec; the cell resistance was 6 megohms; the sensitivity was 1.5×10^{4} volts/watt; and the noise equivalent power (at 5 cps) was ca. 3×10^{-11} watts. The associated electronics did not increase the rise time. The output of the detector was fed into a preamplifier and then to an oscilloscope. The cell was mounted in a turret setting with three-way movement for focussing. A germanium filter cut off radiation below 2.0 μ and the pyrex wall of the shock tube absorbed radiation larger than 2.8 μ. In addition, a Corning filter No. 3484 with a long wave length cut off at 2.6 μ was used. This effectively isolted radiation from the 0 → 2 transition in carbon monoxide which is centered at 2.335 μ. In control experiments with dry nitrogen, less than 4 percent emission was observed. The experimental layout is shown in Fig. 1.

Fig. 1 here

This also shows schematically the schlieren systems which were used for starting and stopping the timer and triggering the oscilloscopes.

The removal of impurities. Early work served to emphasize the importance of excluding water vapor and other impurities from the system due to the very high efficiency of these molecules as collision partners for the relaxation process. Two measures were necessary: (a) the use of carbon monoxide of very high purity, (b) the reduction of the static pressure of H_2O or CO_2 in the shock tube, caused by desorption from the walls, to as low a level as possible.

One series of experiments was made with Matheson Assayed Reagent Grade CO. Mass spectrometric analyses were supplied and listed the main impurities in two samples as carbon dioxide, 0.04 and 0.27 mole percent, and hydrogen, 0.03 and 0.02 mole percent. Most of the work was done with samples prepared by fractional distillation of Matheson C.P. grade carbon monoxide in a good low temperature column with a reflux head refrigerated with pumped down liquid nitrogen. This gave quite pure CO. A typical mass spectrometer analysis (Consolidated Electrodynamics Co.) is: O_2, 10^{-4} mole percent, H_2O, less than .015 mole percent, all other impurities less than .005 mole percent.

The other source of impurities was the walls of the shock tube. To combat this three measures were adopted. (a) The whole low-pressure section of the shock-tube, except for the observation area, was wound with a heating element. A temperature of 50 to 70°C could then be maintained while pumping out the tube to facilitate outgassing. (b) A false end-plate was designed fitted with a re-entrent cold finger which could be refrigerated with liquid nitrogen or other coolant. During evacuation a hole in the false end-plate gave access from the main volume of the tube to the cold finger which lay between the true end and the false end. Before starting a run, this hole was filled by pushing in a plug, the shaft of which extended through the tube end-plate via a hole sealed with an O-ring. The end-plate also carried a mounting for a Phillips ionization gauge. (c) The pumping arrangements for the tube, which now has a volume of about 80 liters, were improved by installing a three-stage oil diffusion pump connected to the tube via a high-speed, one-inch aperture baffle valve.

With the aid of these improvements, it was possible to achieve a pressure of about 10^{-5} mm Hg with liquid nitrogen in the cold finger. The pressure rise with the shock-tube isolated was less than 10^{-6} mm per minute. Since a run takes about 10 minutes, this is negligible with the amounts of gas used. For experiments with added CO_2, the cold finger was filled with dry ice and trichlorethylene, and a control experiment was made under these conditions without added CO_2. Mixtures of CO and CO_2 were made up beforehand in a storage bulb. For experiments with added H_2O, either dry ice as above or methylene bromide at its freezing point was employed. The technique adopted was to admit excess water vapor to the tube first and then let in the CO. About 15 minutes was allowed for the H_2O to come to equilibrium with the ice on the cold finger and to mix with the CO. The vapor pressure of H_2O is 0.56 μ at -78°C (dry ice) and about 50 μ at -50°C (melting methylene bromide). Control runs without added H_2O were done at each temperature.

Calculation of Temperature and Pressure. The temperature and density of a shocked gas can be calculated from the shock velocity and the initial conditions if the enthalpy of the gas is known as a function of temperature. As vibrational relaxation occurs behind a strong shock, the temperature decreases and the density increases. The situation is more complicated for reflected shocks. We have calculated the conditions behind the reflected shock from the measured velocity of the incident shock. We assume, in accordance with the evidence, that the gas behind the incident shock is unrelaxed. Calculations have been made for the unrelaxed incident -

unrelaxed reflected condition. This is strictly applicable to the reflected shock very close to the end plate. Calculations could also be made for the unrelaxed incident-relaxed reflected conditions. This would be appropriate for the steady state shock after a long period of time. One is however observing the process of vibrational relaxation close to the end plate. Neither of the above limiting steady flow conditions therefore applies. The gas behind the shock is contracting and the resulting rarefaction wave is moving out to merge with and slow down the shock. A correct calculation would be very complicated. We have therefore used the unrelaxed-unrelaxed calculations of temperature and density. Fortunately, the vibrational enthalpy is not too large and the uncertainties are small.

Examples of reflected shock calculations are given in Table I.

Table 1. Typical Shock Parameters in CO

T_i °K	S_i cm/msec	π_i	Δ_i	T_r °K	S_r cm/msec	π_r	Δ_r	π_t	Δ_t
500	69.97	4.44	2.65	739	35.13	3.31	2.24	14.7	5.93
600	83.47	6.39	3.18	965	37.72	4.05	2.52	25.9	7.99
700	95.23	8.37	3.57	1192	40.42	4.59	2.70	38.4	9.61
800	105.8	10.36	3.86	1420	43.06	5.01	2.82	51.9	10.89
900	115.4	12.36	4.09	1648	45.61	5.33	2.91	65.9	11.92
1000	124.0	14.36	4.28	1886	48.28	5.60	2.97	80.4	12.70
1100	132.3	16.34	4.43	2120	50.84	5.83	3.02	95.4	13.36
1200	140.2	18.35	4.56	2340	53.77	6.00	3.07	110.0	14.00
1300	147.6	20.36	4.67	2560	54.91	6.14	3.11	124.8	14.50
1400	154.8	22.40	4.77	2800	56.20	6.28	3.14	140.5	14.98
1500	161.6	24.40	4.85	3020	58.38	6.40	3.17	156.0	15.38

T, temperature of heated gas behind shock; S shock velocity; π, pressure ratio across shock; Δ, density ratio across shock. Subscript i refers to incident shock, subscript r refers to reflected shock, and subscript t refers to total change.

Results

The vibrational relaxation time of carbon monoxide has been measured between 1400°K and 3000°K and over a range of final pressures from 1 to 3.5 atm. A preliminary study of the effect of small amounts of CO_2 and H_2O has also been made.

A typical experimental record of infra-red emission due to the 2 → 0 transition is shown in Fig. 2.

Fig. 2 here

As indicated previously, it is believed that the intensity of the emission is directly proportional to the concentration of molecules in the upper state. After a small initial region of gradually increasing slope, the trace rises almost linearly for about half the total amplitude and then approaches the equilibrium value asymptotically.

Interpretation. One may conceive of any one of three possibilities as being the most important path for populating the state $v = 2$.

There is the direct 0 → 2 excitation

$$CO + CO \underset{k_{20}}{\overset{k_{02}}{\rightleftharpoons}} CO + CO^{**} \qquad (1)$$

There is a two step process, 0 → 1 → 2.

$$CO + CO \underset{k_{10}}{\overset{k_{01}}{\rightleftharpoons}} CO^{*} + CO \qquad (2)$$

$$CO^{*} + CO \underset{k_{21}}{\overset{k_{12}}{\rightleftharpoons}} CO^{**} + CO$$

There is also the possibility (3), in which two CO^{*} molecules react to give $CO^{**} + CO$, in which no conversion of translational energy to vibra-

tional energy occurs, but in which the vibrational energy is redistributed. For this process the forward and reverse rate constants, $\underline{e}$, are equal.

$$CO + CO \underset{\underline{k}_{10}}{\overset{\underline{k}_{01}}{\rightleftharpoons}} CO^{*} + CO \qquad (3)$$

$$CO^{*} + CO^{*} \underset{\underline{e}}{\overset{\underline{e}}{\rightleftharpoons}} CO^{**} + CO \qquad (3a)$$

For simplicity, make the approximation $(CO^{**}) \ll (CO^{*}) \ll (CO)$. Hypothesis (1) gives a simple exponential growth of (CO^{**}).

$$(CO^{**}) = (CO^{**})_{\infty} \left\{1 - \exp\left[-\underline{k}_{20}(CO)\underline{t}\right]\right\} \qquad (1a)$$

In the harmonic oscillator exproximation, $\underline{k}_{12} = 2\underline{k}_{01}$, $\underline{k}_{21} = 2\underline{k}_{10}$. Then hypothesis (2) gives

$$(CO^{**}) = (CO^{**})_{\infty} \left\{1 - \exp\left[-\underline{k}_{10}(CO)\underline{t}\right]\right\}^{2} \qquad (2a)$$

If in hypothesis (3), we assume $\underline{e}$ is very large, expression (2a) again results. Thus, (1) gives a simple exponential growth, beginning with a finite slope, whereas (2) and (3) give growth beginning with zero slope, then rising steeply, with a rise time of the order of $1/\underline{k}_{10}(CO)$, namely the relaxation time of the first vibrational state.

Hypothesis (3) can be discussed in further detail as follows. Reactions like (3a) are "energy transfers at exact resonance." The complete set of such reactions do not create vibrational energy, but they redistribute it in such a way that the population of the n'th level, (CO^{n*}), is related to the population of the first excited level by

$$(CO^{n*}) = (CO^{*})^{n} \left(\frac{\underline{E}_{vib}}{\underline{h\nu} + \underline{E}_{vib}}\right) \left(\frac{\underline{h\nu}}{\underline{h\nu} + \underline{E}_{vib}}\right)$$

That is, there is a Boltzmann-like distribution determined by the total amount of vibrational energy, E_{vib}, in the system. Given such a Boltzmann-like distribution, reactions like (3a) will be proceeding backward and forward at equal rates and will not further affect the distribution. Now, Montroll and Shuler[9] have shown that if one considers the complete set of equations like (2) in the harmonic oscillator approximation, then a system which starts with a Boltzmann distribution of vibrational states appropriate to one temperature relaxes to the Boltzmann distribution appropriate to the translational temperature via a set of Boltzmann distributions appropriate to intermediate temperatures. Under these circumstances, the reaction system (3a) makes no contribution to the vibrational distribution even though its rate constant may be large.

Plots of $\ln\left\{1 - (CO^{**})/(CO)^{**}_{\infty}\right\}$ vs. t and of $\ln\left\{1 - \left[(CO^{**})/(CO^{**}_{\infty})\right]^{1/2}\right\}$ vs. t are shown in Fig. 3. The latter relation gives a better straight line, thus favoring hypothesis (2) or (3). The situation is not perfectly

Fig. 3 here

clear cut however because the finite rise time of the detector tends to make a curve like (1a) look like (2a). We believe this effect is small. A more detailed examination of this point will be made in a later paper.

Accept equation (2a). Define the relaxation time, τ, as $1/k_{10}(CO)$. From the equation there is a point of inflection, $d^2(CO^{**})/dt^2 = 0$ at $(CO^{**}) = (CO^{**})_{\infty}/4$. On both sides of this point, the curve is almost linear and the slope is $2/\tau$. Values of τ so obtained are presented in Table 2.

Table 2. Relaxation Time Measurements

Initial Pressure of CO atm	T_i °K	T_r °K	π_t	Δ_t	P_r atm	τ μsec	τP_r μsec atm
.0560	810	1446	53.7	11.01	3.01	278	836
.0483	810	1446	53.7	11.01	2.62	246	645
.0718	767	1395	50.6	10.77	3.63	168	610
.0469	814	1453	54.2	11.04	2.54	237	601
.0311	811	1447	53.7	11.01	1.67	352	588
.0484	805	1433	52.9	10.95	2.56	224	573
.0318	815	1455	54.3	11.05	1.73	327	565
.0317	810	1445	53.6	11.00	1.70	325	552
.0403	812	1451	54.0	11.03	2.18	248	540
.0306	835	1500	57.0	11.28	1.74	234	407
.0248	930	1724	70.3	12.19	1.74	183	319
.0182	1112	2150	97.6	13.54	1.78	132	234
.0216	1012	1916	82.3	12.84	1.78	98	174
.0215	1015	1921	82.7	12.87	1.78	97	172
.0179	1122	2170	98.9	13.60	1.77	67	119
.0181	1100	2117	95.4	13.45	1.73	66	104
.0062	1485	2985	153.0	15.33	0.95	37	35
.0060	1485	2985	153.0	15.33	0.92	37	34

The mean value of the measurements in the vicinity of 1400°K, converted to 1400°K and 1 atm pressure, is

$$\tau = 650 \pm 50 \text{ microseconds}$$

The form of pressure and temperature dependence used in making these conversions will be discussed below. τ may also be obtained from the slope of the straight line in Fig. 3 which has the advantage of using the whole curve. Within the limits of accuracy both methods gave the same results in several cases and the less laborious inflection point method was therefore adopted.

Pressure dependence of τ. For a collisional process, a simple inverse pressure dependence is to be expected. A graph of τp versus p for those experiments close to 1400°K is shown in Fig. 4. The values of τ have been converted to 1400°K. A reasonable fit to a straight line is obtained.

Fig. 4 here

Temperature dependence of τ. The relaxation times are observed to decrease with increasing temperature as expected. The usual theories of vibrational relaxation lead to an expression of the form,

$$\log \tau = AT^{-1/3} + B \qquad (4)$$

where A and B are constants. Values of $\log \tau$ versus $T^{-1/3}$ for the present observations are plotted in Fig. 5. The best straight line that

Fig. 5 here

can be drawn through the experimental points leads to $A = 64.45$ and $B = -2.943$

Equation (3) and the above value of A were used in making the conversions of τ to 1400°K mentioned earlier.

The effect of impurities. The effect of small amounts of added H_2O or CO_2 on the relaxation time of CO is shown in Table 3. Water causes

Table 3. Effect of Impurities on Vibrational Relaxation of CO

Composition of gas	Coolant in Trap	T_r °K	P_r atm	τ μsec	τP μsec atm
pure CO*	dry ice	1437	1.74	198	344
pure CO*	melting methylene bromide	1437	1.72	210	361
CO + .002% H_2O	dry ice	1393	1.61	212	341
CO + .3% H_2O	melting methylene bromide	1430	1.70	35	60
CO + .1% CO_2	dry ice	1431	1.70	150	255
CO + .03% H_2 with < .04% CO_2	liq N_2	1404	1.24	178	220

*Control runs with pure gas.

a marked increase in the rate of relaxation even in trace amounts. At a relative concentration of 3 parts in 10^3 the value of τ is reduced by at least a factor of six. The reduction may be somewhat greater because the observed time is close to the response time of the detector. For CO_2 a ratio of 1 part in 10^3 reduces τ by about a factor of two-thirds. The experiment with the Matheson Reagent Grade CO gave relaxation times of about half those observed with the fractionally distilled samples. Since the CO_2 impurity was removed by the -196°C trap, this may be due to the hydrogen impurity.

Conclusions

1. The value reported here, τ = 550 μsec at 1470°K, is 30 times greater than that given in our preliminary report.[4] The value at 2200° (150 μsec) is greater than the value of 10 μsec given in a preliminary report by the Princeton group.[8] This is presumably a matter of the removal of impurities. It is of course possible that even the present results are effected by impurities.

At present one may say that CO has the longest vibrational relaxation times known at any given temperature.

2. The experimental data favor hypotheses (2) and/or (3) over (1). Theory very strongly seconds the motion,[1] in that the interconversion of a large amount of energy between vibration and translation, as in reaction (1), is predicted to be extremely improbable ($\sim 10^{-7}$ less probable than process (2) in the present instance).

We have made preliminary calculations of the rate constants k_{10} and e for equations (2) and (3) above according to the Schwartz, Slawsky, Herz-

field theory[1] as amended by Tanczos.[10] For the Lennard-Jones parameter, σ, for CO, we use 3.59 Å.[11] We calculate, at 1400°K, $k_{10} = 1.9 \times 10^{-6}$ Z, $k_{01} = 2.1 \times 10^{-7}$ Z, $e = 4.3 \times 10^{-3}$ Z. Z is the gas kinetic theory collision number. The experimental τ at 1400°K corresponds to $k_{10} = 5 \times 10^{-7}$ Z. The agreement between theory and experiment is as good as can be expected. Note that although e is calculated to be about 10^3 greater than k_{10}, the discussion given earlier indicates that the energy transfer at exact resonance probably does not affect the kinetics of the population of the various vibrational states significantly.

3. The vibrational relaxation time of CO is greatly diminished by the impurities H_2O and CO_2. These molecules have shorter vibrational relaxation times, and we suggest that the principal process is the highly efficient transfer of vibrational energy from one species to the other: $H_2O^* + CO \rightleftharpoons H_2O + CO^*$.

4. The infrared method for measuring vibrational relaxation times has the advantage of looking, at least to some extent, at the rate of excitation of particular states. The limitations as to rise time and sensitivity of detectors presently available are such that the method is applicable only to infra-red active molecules with rather long relaxation times.

Acknowledgments

We are indebted to the ONR for support. Dr. Russ Duff of Los Alamos generously performed many of the reflected shock calculations.

One of us (M.W.) is indebted to the Commissioners for the Exhibition of 1851 for a Senior Studentship, and one of us (R.T.) is indebted to the duPont Co. for a fellowship.

Contribution No. 2330 from the Gates and Crellin Laboratories of Chemistry

References

1. K. Herzfeld, Thermodynamics and Physics of Matter, Princeton University Press, 1955, Section H, p. 646.
2. V. Blackman, J. Fluid Mech. 1, 61 (1956)
3. P. V. Slobodskaya, Izvest. Akad. Nauk. S.S.R., Ser. fiz. 12, 656 (1948)
4. M. W. Windsor, N. Davidson and R. Taylor, J. Chem. Phys. 27, 315 (1957)
5. S. Penner and D. Weber, J. Chem. Phys. 19, 807, 817 (1951)
6. S. Penner and D. Weber, J. Chem. Phys. 19, 1351, 1361 (1951)
7. D. Britton, N. Davidson and G. Schott, Discussions of the Faraday Society, No. 17, 1954, pp. 58-68
8. W. D. Greenspan and V. H. Blackman, Bull. Am. Phys. Soc. 112, 217 (1957) (April 1957, Washington meeting)
9. E. Montroll and K. E. Shuler, J. Chem. Phys. 26, 454 (1957)
10. F. I. Tanczos, J. Chem. Phys. 25, 439 (1956)
11. J. O. Hirschfelder, C. F. Curtiss, and R. B. Bird, Molecular Theory of Gases and Liquids, J. Wiley and Sons, Inc., New York, 1954, p. 1111
12. S. J. Lukasik and J. E. Young, J. Chem. Phys. 27, 1149 (1957)
13. H. and L. Knötzel, Ann. Physik 2, 393 (1948)
14. P. W. Huber and A. Kantrowitz, J. Chem. Phys. 15, 275 (1947)

Legends for Figures

Fig. 1. Schematic Diagram of Equipment.

Fig. 2. Typical Oscillograph Record of Emission from CO heated by Shock. Initial condition; $\underline{T}$ = 298°K; $\underline{P}$ = .056 atm CO. Final condition, $\underline{T}$ = 1446°K, $\underline{P}$ = 3.01 atm. Time is the horizontal coordinate. The three horizontal sweeps at the top, middle, and bottom of the picture are time calibration marks with 100 μsec pips. Emission of CO increeases vertically.

Fig. 3. One-step versus Two-step Relaxation Processes.

Fig. 4. Pressure Dependence of Vibrational Relaxation in CO.

Fig. 5. Temperature Dependence of Vibrational Relaxation in CO.

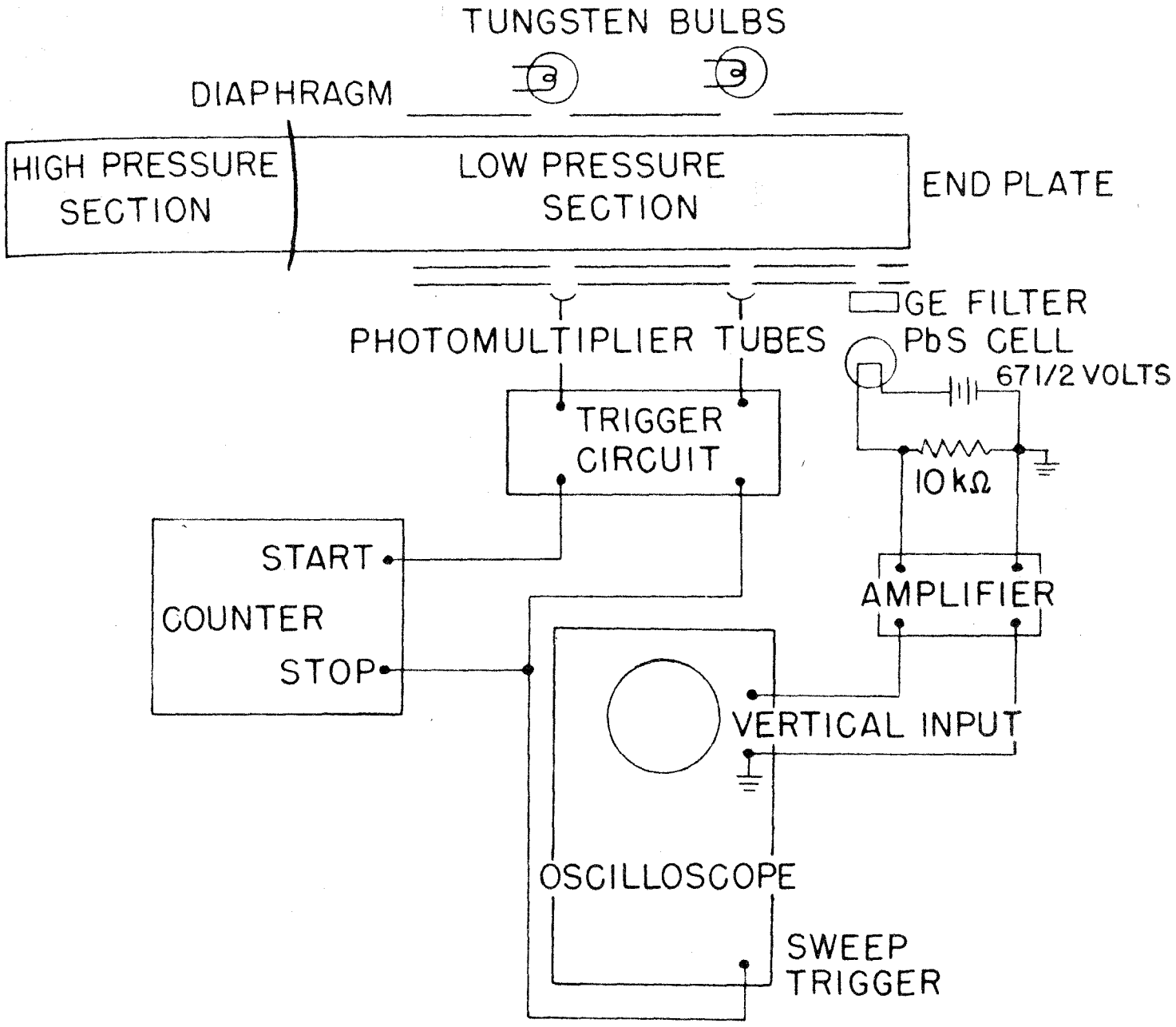
TUNGSTEN BULBS
DIAPHRAGM
HIGH PRESSURE SECTION
LOW PRESSURE SECTION
END PLATE
GE FILTER
PbS CELL
PHOTOMULTIPLIER TUBES
67 1/2 VOLTS
TRIGGER CIRCUIT
10 kΩ
START
COUNTER
STOP
AMPLIFIER
VERTICAL INPUT
OSCILLOSCOPE
SWEEP TRIGGER

Fig. 1

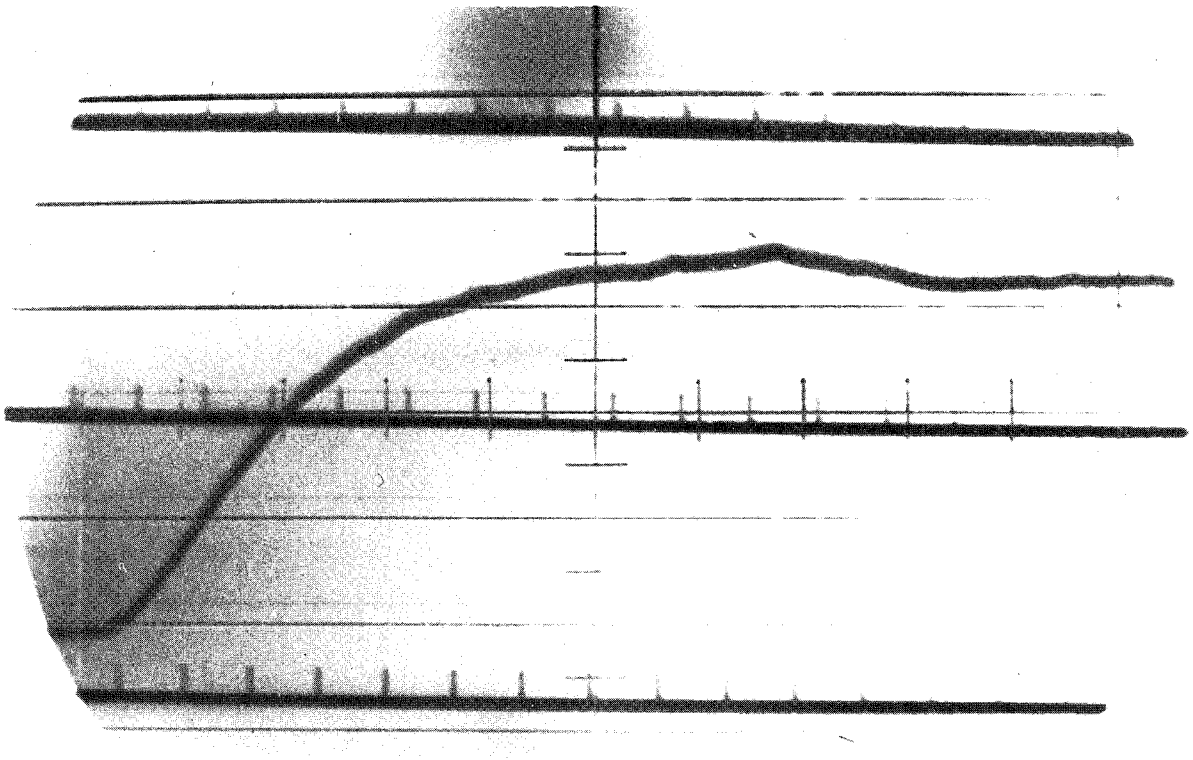

Fig. 2

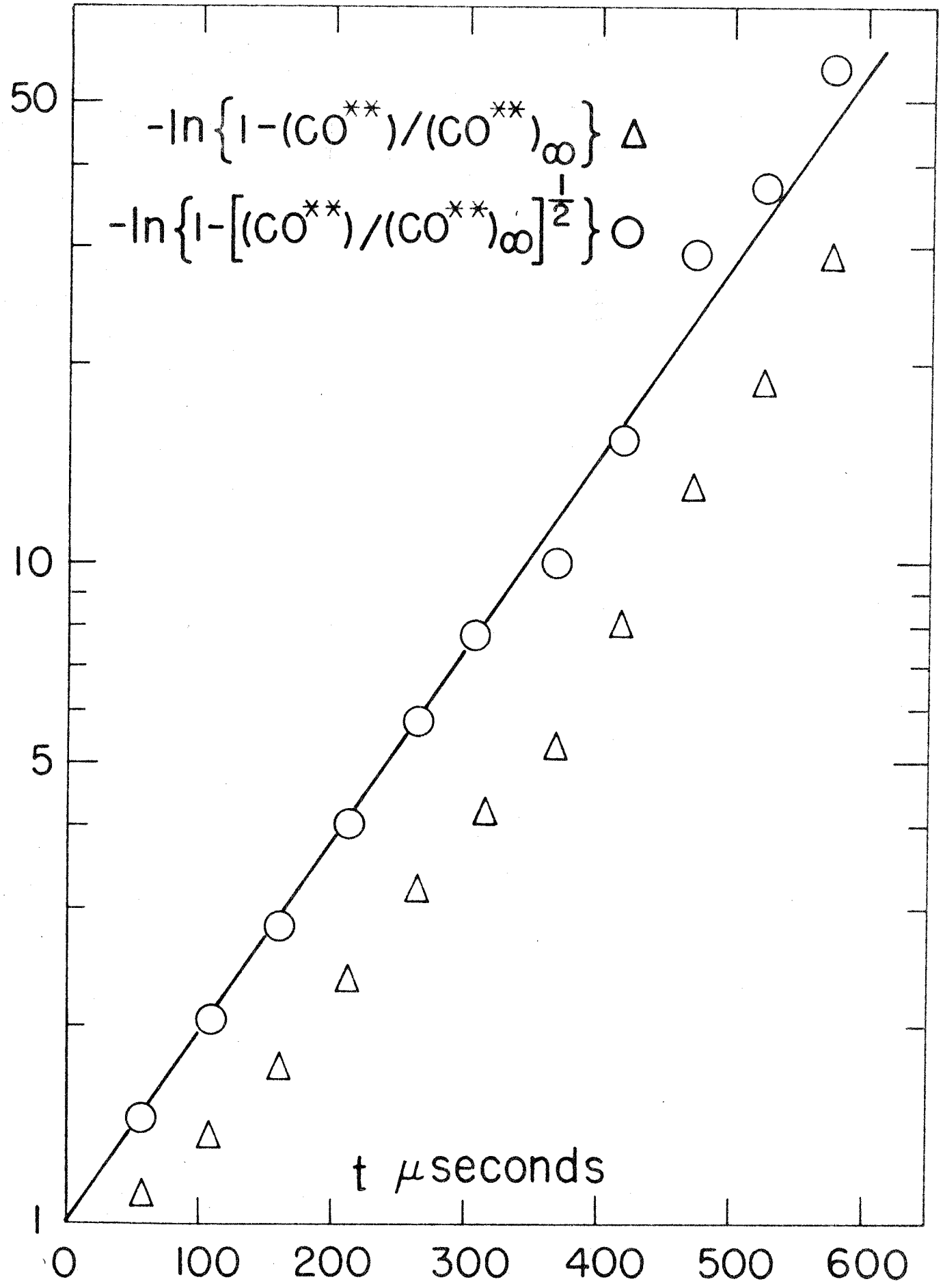
50
10
5
1
$-\ln\{1-(CO^{**})/(CO^{**})_\infty\}$ Δ
$-\ln\{1-[(CO^{**})/(CO^{**})_\infty]^{\frac{1}{2}}\}$ O
t μseconds
0
100
200
300
400
500
600

Fig 3

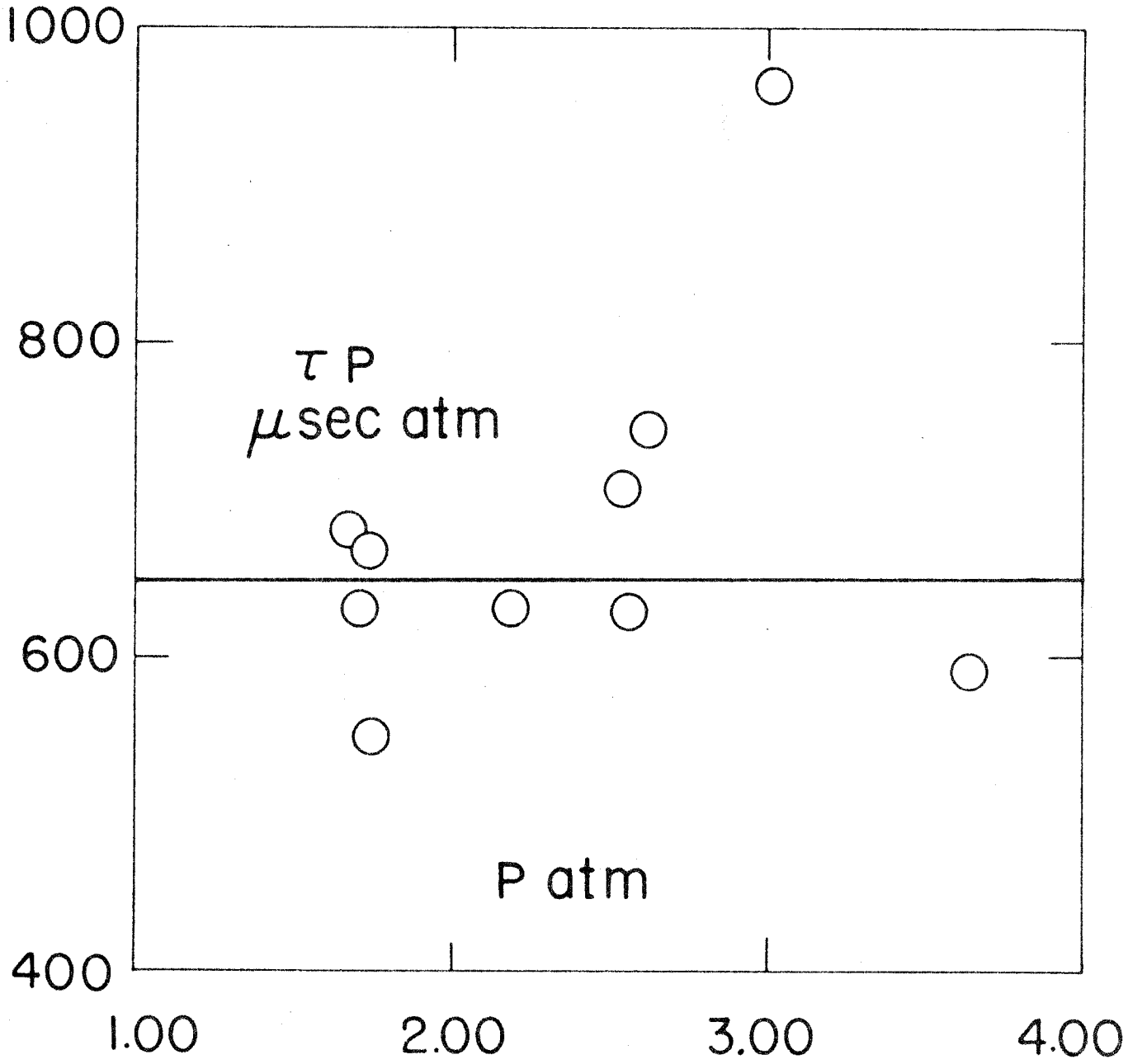

Fig. 4

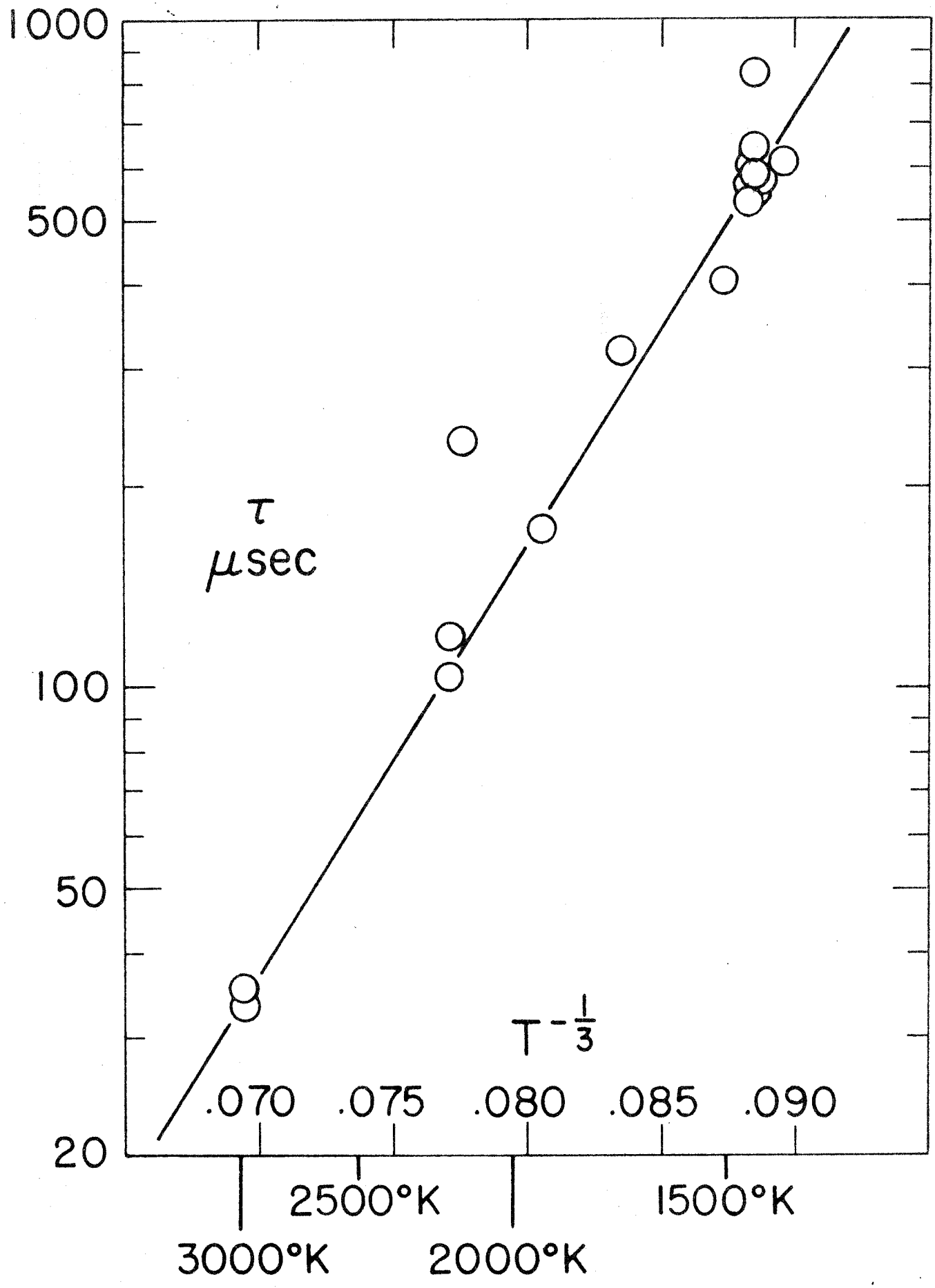
1000
500
100
50
20
τ
μsec
T^-1/3
.070
.075
.080
.085
.090
2500°K
1500°K
3000°K
2000°K

Fig 5

APPENDIX

A Comparison of Experimental and Theoretical Relaxation Times in Carbon Monoxide, Nitrogen, and Oxygen

Since carbon monoxide, nitrogen, and oxygen have been studied experimentally over the widest range of temperature, they offer the best available data for a test of present molecular theories of vibrational energy exchange. The experimental values of relaxation times of carbon monoxide obtained in this investigation are reproduced in Figure 6 and compared with the values predicted by the Schwartz, Slawsky, and Herzfeld[1] theory. Also shown are experimental and theoretical values for nitrogen and oxygen.

For nitrogen the experimental relaxation times in the temperature range 3500 - 5000°K are due to Blackman,[2] in the range 800 - 1200°K to Lukasik and Young,[12] and at lower temperatures to Huber and Kantrowitz[14]. For oxygen all the data are from Blackman's experiment except for the room temperature result of H. and L. Knötzel[13].

The agreement between theory and experiment for these three gases is good except at the lower temperatures, principally below 1000°K. The presence of small amounts of polyatomic impurities is expected to be more important in decreasing the relaxation times at lower temperatures and may be the reason for the discrepancy between theory and experiment in this region.

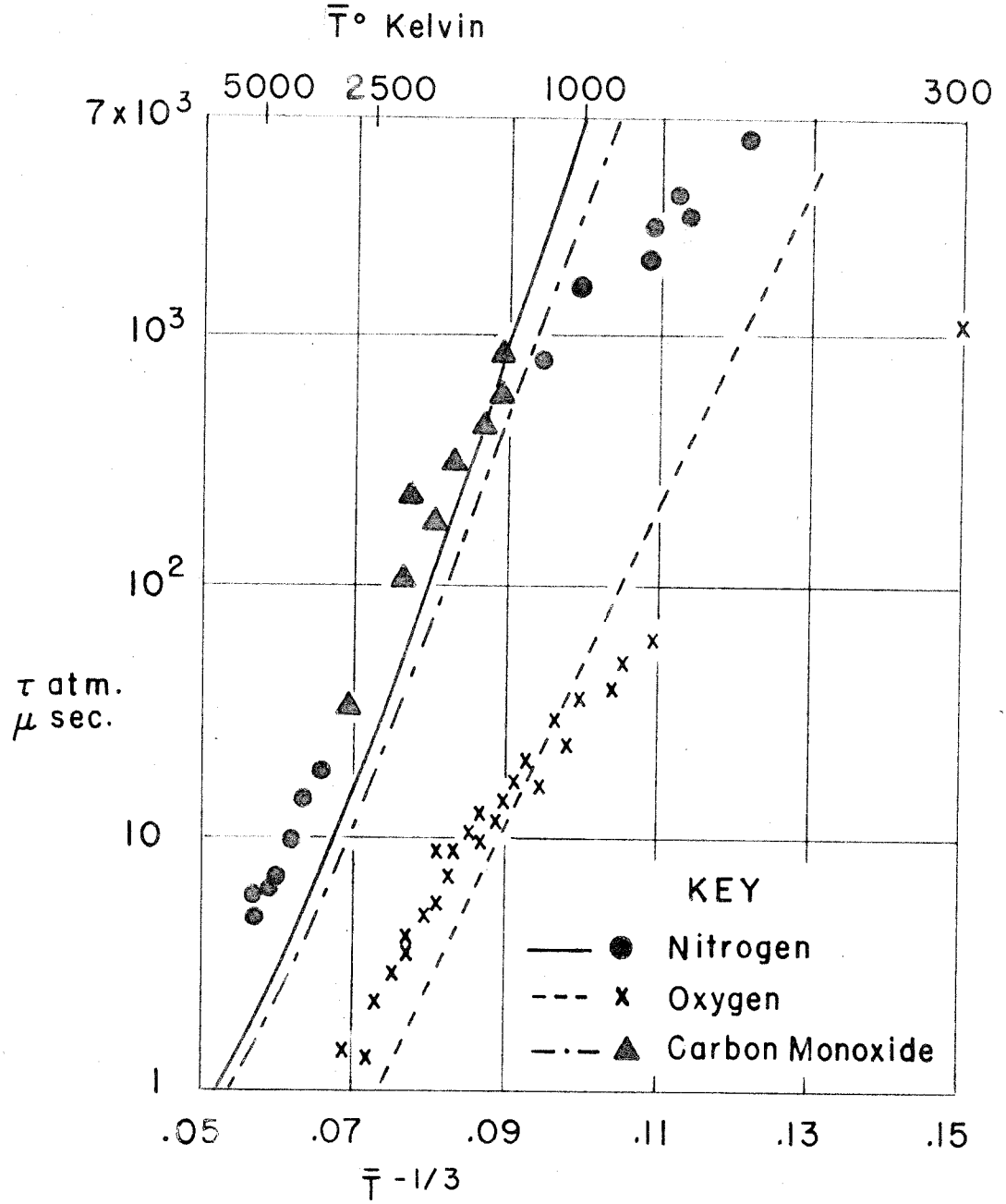

Fig. 6 — Relaxation times in N_2, O_2, and CO.

II. THE EFFECT OF RESONANT ENERGY EXCHANGE IN THE VIBRATIONAL RELAXATION OF GAS MIXTURES

Introduction

The exchange of energy between the vibrational motion of one molecule and the translational or rotational motion of a second molecule during a collision is the principal process for the vibrational relaxation of a pure gas. However, a second possibility arises in a collision between unlike molecules in which vibrational energy is transferred directly between the molecules with little or no energy being exchanged with translation. Such a process is called a resonant or near-resonant transfer of energy. If the vibrational frequencies of the molecules are identical or nearly so, the process is one of exact resonant transfer. Otherwise, it is a near-resonant process, and some energy must also be exchanged with the relative translational motion of the collision pair. The molecular theory of vibrational energy exchange predicts that resonant and near-resonant processes are, in general, more probable than the direct excitation of vibrations from translational motion. These latter collisional processes are called non-resonant transitions.

Schwartz, Slawsky, and Herzfeld (1) were perhaps the first to examine the importance of resonant-like mechanisms in the vibrational relaxation of gas mixtures. They indicated that the resonant mechanism might be important in several systems, but no detailed calculations of the magnitude of the expected effect were given.

The present investigation is a study of the vibrational relaxation of a two component gas in which both resonant and non-resonant processes are allowed. The macroscopic relaxation equations for the vibrational energy of the component gases are developed in a manner analogous to that of Schwartz et al., but a specific numerical calculation is carried out for oxygen and nitrogen mixtures. These gases were chosen because: (a) the fundamental vibrational frequencies, O_2 - 1580 cm^{-1} and N_2 - 2360 cm^{-1}, are close enough to enable the near-resonance process to assume importance, (b) the vibrational relaxation of the pure gases has been extensively studied experimentally, and (c) these molecules are relatively simple, and, therefore, a reasonably meaningful calculation of the probabilities of energy exchange is possible from present theory.

Macroscopic Relaxation Equations

<u>One Component System</u>. The equation describing the relaxation of the vibrational energy of a one component gas composed of diatomic molecules has been thoroughly discussed in the literature (2). For the rate of change of the total vibrational energy, E_{vib}, one obtains:

$$\frac{dE_{vib}}{dt} = -k_{10}(1 - e^{-\Theta})(E_{vib} - \bar{E}_{vib}) \qquad (1)$$

k_{10} is the rate of deactivation of a molecule from the first excited vibrational level, $\Theta = h\nu/kT$ where these symbols have their usual meanings, and $\bar{E}_{vib}$ is the vibrational energy of the system at equilibrium.

This relation is derived with the following basic assumptions: (a) the molecules are considered to be harmonic oscillators, (b)

only energy transfer between neighboring levels is allowed, and (c) the rates of energy transfer obey the same selection rules as the optical transitions of harmonic oscillators. The last two assumptions are a consequence of the quantum mechanical calculation of the molecular process of energy transfer and are formally known as the Landau - Teller selection rules (2).

Since energy is being transferred between the translational and vibrational modes during the relaxation process, the translational temperature, T, and the equilibrium energy, $\bar{E}_{vib}$, may not be strictly constant with time. In many practical problems this effect is small and in theory can be made negligible through the use of a temperature buffer such as a large excess of inert gas. With the assumption of a constant translational temperature equation 1 can be integrated to yield

$$E_{vib} = \bar{E}_{vib}\left(1 - e^{-t/\tau}\right) \tag{2}$$

where the time constant, τ, defined as

$$\tau = \frac{1}{k_{10}(1 - e^{-\theta})} \tag{3}$$

has been introduced.

For a one component system of harmonic oscillators one obtains the result that the vibrational energy relaxes toward its equilibrium value exponentially with a tim e constant given essentially by the reciprocal of the rate of deactivation of the first excited level.

Two Component System. The macroscopic relaxation equations equivalent to 1 for a system of two gases, each of which has one vibrational mode, have been derived by Schwartz, Slawsky and Herzfeld (1). The following derivation is more detailed and differs in some

respects from the one presented by these authors.

In the notation of chemical kinetics the two different energy transfer processes are expressed as follows:

Non-resonant energy transfer

$$A^* + M \rightleftharpoons A + M \qquad (4)$$
$$B^* + M \rightleftharpoons B + M$$

Resonant or near-resonant energy transfer

$$A^* + B \rightleftharpoons A + B^* \qquad (5)$$

The starred symbols represent vibrationally excited molecules.

In equations 4 symbol M represents either an A or B type molecule. The assumption is being made that the rates of the non-resonant processes such as 4 are the same whether the collisions are with an A or B molecule. For the specific problem of oxygen and nitrogen this assumption is approximately true, and the use of an average molecule M is convenient. The equations could, if necessary, be derived for the more general case.

The bimolecular rate constants for equations 4 and 5 are composed of two factors - a collision frequency, Z, and a probability of energy exchange per collision, P. These are defined in detail as follows:

$Z_{A,B}$ is the number of collisions per second per A molecule if one considers that all of the rest of the gas is composed of B molecules and is given by the kinetic theory expression

$$Z_{A,B} = \sqrt{\frac{8\pi^2 k T}{\mu}}\ \sigma_{A,B}^2\ \frac{P}{k T} \qquad (6)$$

where P is the total pressure, and the other symbols have their usual meanings. $Z_{A,M}$ is the number of collisions per second per A molecule with all the molecules M when the total pressure is P. A similar definition exists for $Z_{B,M}$.

$P(A,M)^{i+1,\,i}$ is the probability per collision that molecule A in the $(i+1)$th quantum state will be deactivated to the ith quantum state in a non-resonant process. Similar definitions hold for $P(B,M)^{j+1,\,j}$ and the probabilities for activation, $P(A,M)^{i,\,i+1}$ and $P(B,M)^{j,\,j+1}$.

$P(A,B)^{i+1,\,i}_{j,\,j+1}$ is the probability per collision that A is deactivated from the $(i+1)$th to the ith quantum state in a resonant or near-resonant collision with molecule B which in turn is activated from the jth to the $(j+1)$th state. An analogous definition exists for the inverse process, $P(B,A)^{j+1,\,j}_{i,\,i+1}$.

Let A_i represent an A molecule in the ith vibrational state and n_i the population of such molecules; similarly B_j is a B molecule in the jth vibrational state and m_j the population of B_j molecule. The total number of molecules, N, in the mixture is given by

$$N = \sum_i n_i + \sum_j m_j \tag{7}$$

The fraction of A or B type molecules is designated as a or b respectively. There are obvious relations

$$a = \frac{\sum_i n_i}{N}$$

$$b = \frac{\sum_j m_j}{N} \tag{8}$$

Rate equations of the type 4 and 5 for the individual vibrational levels can be written in terms of the above definitions.

Considering the A type molecules alone these equations are

$$\left.\begin{array}{lll} A_0 + M & \underset{P(A,M)^{10}}{\overset{P(A,M)^{01}}{\rightleftharpoons}} & A_1 + M \\ A_1 + M & \underset{P(A,M)^{21}}{\overset{P(A,M)^{12}}{\rightleftharpoons}} & A_2 + M \\ \vdots & & \\ A_i + M & \underset{P(A,M)^{i+1,i}}{\overset{P(A,M)^{i,i+1}}{\rightleftharpoons}} & A_{i+1} + M \end{array}\right\} \quad (9)$$

$$\left.\begin{array}{lll} A_0 + B_1 & \underset{P(A,B)^{10}}{\overset{P(A,B)^{01}}{\rightleftharpoons}} & A_1 + B_0 \\ A_1 + B_1 & \underset{P(A,B)^{21}}{\overset{P(A,B)^{12}}{\rightleftharpoons}} & A_2 + B_0 \\ \vdots & & \\ A_i + B_1 & \underset{P(A,B)^{i+1,i}}{\overset{P(A,B)^{i,i+1}}{\rightleftharpoons}} & A_{i+1} + B_0 \end{array}\right\} \quad (10)$$

$$\left.\begin{array}{lll} A_0 + B_2 & \underset{P(A,B)^{10}}{\overset{P(A,B)^{01}}{\rightleftharpoons}} & A_1 + B_1 \\ A_0 + B_3 & \underset{P(A,B)^{10}}{\overset{P(A,B)^{01}}{\rightleftharpoons}} & A_1 + B_2 \\ \vdots & & \\ A_0 + B_{j+1} & \underset{P(A,B)^{j,j+1}}{\overset{P(A,B)^{j+1,j}}{\rightleftharpoons}} & A_1 + B_j \end{array}\right\} \quad (11)$$

The set of equations 9 describes the non-resonant relaxation of A molecules. There is an equivalent set for the non-resonant relaxaction of the B molecules. Equations 10 and 11 describe the resonant transfer of energy between A and B. The rate constants for all these equations have been written in terms of the probabilities, P,

the appropriate collision frequencies being understood. In anticipation of the Landau - Teller selection rules only the equations describing transitions between neighboring vibrational levels have been allowed.

From equations 9, 10 and 11 the rate of growth of the vibrational energy can be expressed as a sum of terms for activation minus a sum of terms for deactivation. Each term is the product of the concentrations of the levels concerned and the rate constant for the process

$$\frac{d(a E_A)}{dt} = N h \nu_A \left\{ Z_{A,M} \left[P^{01}_{(A,M)} \frac{n_0}{N} \frac{M}{N} + P^{12}_{(A,M)} \frac{n_1}{N} \frac{M}{N} + \cdots \right.\right.$$

$$\cdots + P^{i,i+1}_{(A,M)} \frac{n_i}{N} \frac{M}{N} + \cdots - P^{10}_{(A,M)} \frac{n_1}{N} \frac{M}{N} - P^{21}_{(A,M)} \frac{n_2}{N} \frac{M}{N} - \cdots$$

$$\left.\left. \cdots - P^{i+1,i}_{(A,M)} \frac{n_{i+1}}{N} \frac{M}{N} \cdots \right] \right\} \qquad (12)$$

$$+ N h \nu_A \left\{ Z_{A,B} \left[P^{01}_{10(A,B)} \frac{n_0}{N} \frac{m_1}{N} + P^{12}_{10(A,B)} \frac{n_1}{N} \frac{m_1}{N} + \cdots \right.\right.$$

$$\cdots + P^{i,i+1}_{10(A,B)} \frac{n_i}{N} \frac{m_1}{N} + \cdots - P^{10}_{01(A,B)} \frac{n_1}{N} \frac{m_0}{N} - P^{21}_{01(A,B)} \frac{n_2}{N} \frac{m_0}{N} \cdots$$

$$\cdots - P^{i+1,i}_{01(A,B)} \frac{n_{i+1}}{N} \frac{m_0}{N} \cdots + P^{01}_{21(A,B)} \frac{n_0}{N} \frac{m_2}{N}$$

$$+ P^{01}_{32(A,B)} \frac{n_0}{N} \frac{m_3}{N} + \cdots + P^{01}_{j+1,j(A,B)} \frac{n_0}{N} \frac{m_{j+1}}{N} + \cdots$$

$$\left.\left. \cdots - P^{10}_{12(A,B)} \frac{n_1}{N} \frac{m_1}{N} - P^{10}_{23(A,B)} \frac{n_1}{N} \frac{m_2}{N} - \cdots - P^{10}_{j,j+1(A,B)} \frac{n_1}{N} \frac{m_j}{N} \cdots \right] \right\}$$

E_A is defined as the vibrational energy of the gas if the gas were composed only of A molecules; aE_a is then the energy due to the fraction, a, of A molecules.

To further simplify equation 12 the various transition probabilities must be related by the use of the Landau - Teller selection rules which are

$$\begin{aligned} P_{(A,M)}^{i+1,i} &= (i+1)\, P_{(A,M)}^{10} \\ P_{(A,M)}^{i,i+1} &= i\, P_{(A,M)}^{01} \\ P_{\substack{(A,B)\\ j,j+1}}^{i+1,i} &= (i+1)(j+1)\, P_{\substack{(A,B)\\ 01}}^{10} \\ P_{\substack{(A,B)\\ j+1,j}}^{i,i+1} &= (i)(j)\, P_{\substack{(A,B)\\ 10}}^{01} \end{aligned} \tag{13}$$

From considerations of detailed balancing there are the further relations

$$\begin{aligned} P_{(A,M)}^{01} &= P_{(A,M)}^{10}\, e^{-\alpha} \\ P_{\substack{(A,B)\\ 10}}^{01} &= P_{\substack{(A,B)\\ 01}}^{10}\, e^{-(\alpha-\beta)} \end{aligned} \tag{14}$$

where

$$\begin{aligned} \alpha &= h\nu_A/kT \\ \beta &= h\nu_B/kT \end{aligned} \tag{15}$$

Using relations 13 and 14 the terms in equation 12 describing the non-resonant relaxation (first set of braces) can be summed to yield

$$Z_{A,M}\, P_{(A,M)}^{10}\left[e^{-\alpha}\sum_i \frac{n_i}{N} - (1-e^{-\alpha})\sum_i i\,\frac{n_i}{N}\right] \tag{16}$$

The total vibrational energy of the A molecules is given by

$$a E_A = h\nu_A \sum_i i\, n_i \tag{17}$$

and at equilibrium $\bar{E}_A$ is expressed by the well known Einstein relation

$$\bar{E}_A = N h\nu_A \frac{e^{-\alpha}}{1 - e^{-\alpha}} \tag{18}$$

By substituting the two preceding relations into 16 and using the definition of fraction, a, of A molecules (relation 8), the non-resonant terms can be transformed into:

$$Z_{A,M} \left\{ P^{10}_{(A,M)}\, a (1 - e^{-\alpha}) \left[\bar{E}_A - E_A\right] \right\} \tag{19}$$

If a = 1 and $Z_{A,M} P^{10}_{(A,M)} = k_{10}$, this quantity is identical to the rate of change of the vibrational energy of a one component gas, equation 1.

Using the Landau - Teller selection rules the resonant terms in equation 12 (second set of braces) can be summed as follows

$$Z_{A,B} P^{10}_{(A,B)_{01}} \left[e^{-(\alpha-\beta)} \sum_i \frac{n_i}{N} \sum_j \frac{j m_j}{N} - (1 - e^{-(\alpha-\beta)}) \sum_i \frac{i n_i}{N} \sum_j \frac{j m_j}{N} - \sum_i \frac{i n_i}{N} \sum_j \frac{m_j}{N} \right] \tag{20}$$

As was the case with the non-resonant terms, this expression can be rewritten using 17 and 18 and the equivalent relations for the vibrational energy of the B molecules, E_B and $\bar{E}_B$.

$$Z_{A,B} \left\{ P^{10}_{(A,B)_{01}}\, ab \left[E_B \left(\frac{\bar{E}_A - E_A}{\bar{E}_B} \right) \left(\frac{1 - e^{-\alpha}}{1 - e^{-\beta}} \right) - E_A \left(\frac{\bar{E}_B - E_B}{\bar{E}_B} \right) \right] \right\} \tag{21}$$

The final result for the rate of change of E_A is the sum of 19 and 21 or

$$\frac{dE_A}{dt} = Z_{A,M} \left\{ P^{10}_{(A,M)} (1 - e^{-\alpha}) \left[\bar{E}_A - E_A\right] \right\} + b Z_{A,B} \left\{ P^{10}_{(A,B)_{01}} \left[E_B \left(\frac{\bar{E}_A - E_A}{\bar{E}_B} \right) \left(\frac{1 - e^{-\alpha}}{1 - e^{-\beta}} \right) - E_A \left(\frac{\bar{E}_B - E_B}{\bar{E}_B} \right) \right] \right\} \tag{22}$$

The effect of the resonant mechanism on the macroscopic relaxation equation is to add on the second, non-linear term to the quantity describing the usual non-resonant relaxation. Equation 22 is equivalent to the macroscopic relaxation equation for a system of mixed gases derived by Schwartz, Slawsky and Herzfeld (1) except for their omission of the factor $(1 - e^{-\alpha})$ in the first term.

In the preceding derivation the assumed model was one of two gases with one vibrational mode each. An equivalent model would be a pure gas with two vibrational modes, A and B. The derivation of the macroscopic equation for this latter case is similar and yields a final equation identical to 22 with b = 1. Tanczos (3) has derived the energy relaxation equation for a gas composed of a general polyatomic molecule. He has also included resonant transitions involving two quanta in one mode, i.e., processes of the type $P^{20}_{01}(A,B)$.

Equation 22 can be rewritten in terms of the reduced variable $E_A/\bar{E}_A$

$$\frac{d\,E_A/\bar{E}_A}{dt} = -\left[Z_{A,M}P^{10}_{01}(A,M)(1-e^{-\alpha}) + b\,Z_{A,B}P^{10}_{01}(A,B)\right]E_A/\bar{E}_A + b\,Z_{A,B}P^{10}_{01}(A,B)\left(\frac{1-e^{-\alpha}}{1-e^{-\beta}}\right)E_B/\bar{E}_B + b\,Z_{A,B}P^{10}_{01}(A,B)\left(\frac{e^{-\alpha}-e^{-\beta}}{1-e^{-\beta}}\right)E_A/\bar{E}_A\;E_B/\bar{E}_B + Z_{A,M}P^{10}_{01}(A,M)(1-e^{-\alpha}) \tag{23}$$

Since the problem is symmetric in A and B, the relaxation equation for E_B is obtained by interchanging the roles of A and B in 23 or

$$\frac{d\,E_B/\bar{E}_B}{dt} = -\left[Z_{B,M}P^{10}_{01}(B,M)(1-e^{-\beta}) + a\,Z_{B,A}P^{10}_{01}(B,A)\right]E_B/\bar{E}_B + a\,Z_{B,A}P^{10}_{01}(B,A)\left(\frac{1-e^{-\beta}}{1-e^{-\alpha}}\right)E_A/\bar{E}_A + a\,Z_{B,A}P^{10}_{01}(B,A)\left(\frac{e^{-\beta}-e^{-\alpha}}{1-e^{-\alpha}}\right)E_A/\bar{E}_A\;E_B/\bar{E}_B + Z_{B,M}P^{10}_{01}(B,M)(1-e^{-\beta}) \tag{24}$$

These two equations describe the relaxation behavior of the total

vibrational energy of a two component gas in which both resonant and non-resonant energy exchange processes are permitted. They form a set of coupled, non-linear equations, and a general solution has not been found.

Molecular Theory of Vibrational Energy Transfer

This section contains a brief resumé of the molecular theory of vibrational energy transfer. It is presented to emphasize the important features of vibrational relaxation which depend upon molecular properties.

In the preceding section the macroscopic relaxation equations were derived in terms of the probability, P, that vibrational energy is exchanged between molecules during a collision. The calculation of this probability in terms of the molecular parameters of the collision pair has occupied the attention of theoreticians for the past thirty years. Both semi-classical and quantum mechanical approaches have been used. C. Zener (4) and later, independently, Landau and Teller (5) discussed the problem classically. Early quantum attempts to describe the process of energy exchange were made by Kallman and London (6), O. K. Rice (7), and again Zener (4). Although these early investigations discovered important general features of vibrational relaxation, one was not able to make detailed calculations for specific molecules. More recently Schwartz, Slawsky and Herzfeld (1) have extended this early work and have made it possible to make calculations in practical problems.

Classical Considerations. The simplest collision to consider is a one-dimensional encounter between a diatomic molecule, B-C and an atom, A.

A ---------- B-C

Rotation of B-C is neglected; all the motion of the system is assumed to take place in the one dimension. For further simplification the interaction between A and B-C is limited to between A and B. Useful intuitive concepts can be obtained by considering the collision in its classical limits.

If the range of intermolecular forces is large compared to the vibrational amplitude of B-C, then the effect of A upon B-C will be exerted primarily upon the center of gravity of the molecule. Since the forces between A and B are of long-range, the molecule has time to adjust its internal force to compensate for the intermolecular force. In this limit there is a quasi-equilibrium between A and B-C during the collision, and there will be no energy exchanged between the translational and vibrational motions. These collisions are called adiabatic; the perturbation is applied slowly compared to the time characteristic of the system.

At the other extreme there is the possibility that the intermolecular forces are of very short range. In a collision A and B now act as hard spheres, and the duration of their contact is infinitely short. Momentum is transferred to B and into the vibrational motion of B-C. Since the range of force is essentially zero, A is able to move out of range of B before B returns in its harmonic motion to once again collide with A. The energy transferred to B-C remains in its vibrational motion. When the perturbation is applied suddenly, the collisions are called non-adiabatic, and the probability of energy exchange is large compared to adiabatic collisions.

In a gas under ordinary conditions the vast majority of the molecular collisions are adiabatic. Therefore, the vibrational transition probabilities should be small. This conclusion is verified by experiment. At room temperature it is found that gas molecules need hundreds to millions of

collisions to exchange vibrational energy with translational motion.

Although the intuitive concepts gained by a classical consideration of molecular collisions are useful, it is obvious that a quantum mechanical treatment is necessary for a detailed picture of the phenomenon of molecular energy exchange.

Quantum Mechanical Theory. In the language of quantum mechanics the collision between A and B-C is discussed as follows: The atom A is described by a plane wave which is scattered by an interaction with B-C. Two types of scattering are possible - elastic and inelastic. In the former no energy transfer occurs, while in the latter energy transfer takes place accompanied by a change in the vibrational state of B-C. The density of particles per unit volume is given by the square of the amplitude of the wave describing these particles. Therefore, the vibrational transition probability is proportional to the ratio of the square of the amplitudes of the inelastically scattered to incident waves.

The motion of the one dimensional collision discussed previously can be described by the coordinates r, between the centers of mass of the colliding pair and s, the internal coordinate of B-C. It is assumed that the motion is separable in these coordinates. Before colliding the state of the system is given by the product wave function

$$\Psi_o^A(r)\,\Psi_i^B(s) \tag{25}$$

where Ψ_o^A describes the incident particle A with relative velocity V_o and Ψ_i^B describes the initial vibrational state of the molecule B-C. After an inelastic collision the system is characterized by a new relative velocity

V_f and a new vibrational state j and is described by the function

$$a_j \Psi_f^A(r) \Psi_j^B(s) \tag{26}$$

where a_j is the amplitude of the scattered wave. The amplitude of the incident wave, 25, is taken to be unity. The translational wave functions $\Psi^A(r)$ and the vibrational wave functions $\Psi^B(s)$ are chosen to be properly normalized.

The number of particles scattered inelastically which pass a unit area per second is given by

$$|a_j|^2 V_f \tag{27}$$

Therefore, the probability of energy exchange becomes

$$P^{ij} = |a_j|^2 V_f / V_o \tag{28}$$

The amplitude of the scattered wave is given by usual perturbation theory as

$$a_j = \frac{4\pi}{h V_f} H_{ij}^{of} \tag{29}$$

where the perturbation matrix element is defined as

$$H_{ij}^{of} = \iint \Psi_o^A \Psi_i^B H' \Psi_f^A \Psi_j^B \, dr\, ds \tag{30}$$

H′ is the interaction energy between A and B-C and is the perturbation on the system which causes the energy transfer.

In the adiabatic collision approximation H′ is assumed to be expressible as a product of functions of the variables r and s.* In this case H_{ij}^{of} can be separated as the product of two integrals

$$H_{ij}^{of} = R_{of} V_{ij} \tag{31}$$

where

$$R_{of} = \int \Psi_o^A \frac{dH}{dr} \Psi_f^A \, dr \tag{32}$$

---

* H' is a function of the distance between A and B-C which can be expressed in terms of r and s. Then H' is expanded in powers of s and only the first power retained (2).

$$V_{ij} = \int \Psi_i^B \, s \, \Psi_j^B \, dS \tag{33}$$

The correct zeroth order wave functions, Ψ^A, for the perturbation integral 32 are solutions to the elastic scattering problem. They are solutions of the Schrödinger equation for a free particle in the potential field H(r)

$$\frac{d^2\Psi_f^A}{dr^2} + \frac{8\pi^2\mu}{h^2}\left[\frac{\mu V_f^2}{2} - H(r)\right]\Psi_f^A = 0 \tag{34}$$

μ is the reduced mass of the collision pair. Jackson and Mott (8) have solved equation 34 by the "method of distorted waves" (9) for the case of an exponential repulsive potential

$$H(r) = Ce^{-\alpha r} \tag{35}$$

The exact form of the repulsive part of an intermolecular energy surface is not known, and the exponential form was chosen to be mathematically convenient. This restriction can be removed to some extent as will be seen later.

Employing the results of Jackson and Mott, R_{of} can be evaluated to yield

$$R_{of} \propto (\theta_o^2 - \theta_f^2)\frac{(e^{\theta_o} - e^{-\theta_f})^{1/2}(e^{\theta_f} - e^{-\theta_f})^{1/2}}{(e^{\theta_o} + e^{-\theta_o} - e^{\theta_f} - e^{-\theta_f})} \tag{36}$$

where

$$\theta_{o,f} = \frac{4\pi\mu V_{o,f}}{\alpha h} \tag{37}$$

It is evident that R varies with the change in linear momentum; as $\theta_f \rightarrow \theta_o$ the change in momentum decreases, and R approaches a maximum. Therefore, those processes are most probable in which the exchange of energy between relative translational motion and internal degrees of freedom is the smallest. This conclusion is equivalent to the adiabatic approximation in the classical limit.

If it is assumed that the high velocity collisions (non-adiabatic) are most likely to cause energy exchange, then these collisions are ones for which

$$\Theta_f , \Theta_o \gg 1 \tag{38}$$

In this limit if $\Theta_f \neq \Theta_o$, R_{of} becomes

$$R_{of} \longrightarrow (\Theta_o^2 - \Theta_f^2)\, e^{-(\Theta_o - \Theta_f)} \tag{39}$$

and as $\Theta_f \longrightarrow \Theta_o \equiv \Theta$, R_{of} approaches a different limit

$$R_{of} \longrightarrow 2\,\Theta \tag{40}$$

To calculate V_{ij} the molecule B-C is assumed to be a harmonic oscillator. The wave functions Ψ^B are the well known Hermite polynomials solutions for this system. This integral 33 is identical to the matrix element for dipole radiation of a harmonic oscillator and, when evaluated, yields the result

$$V_{i,\,i\pm1} = \left[\frac{h(i + 1/2 \pm 1/2)}{8\pi^2 \mu_{BC}\, \nu_B}\right]^{1/2} \tag{41}$$

where μ_{BC} is the reduced mass of the molecule B-C and ν_B is the fundamental vibrational frequency. The Landau-Teller selection rules arise from the above integral.

The extension of these calculations to the in-line collision of two diatomic molecules or to polyatomic molecules can be made. For each normal mode of oscillation a suitable internal coordinate s_n exists together with its harmonic oscillator wave function Ψ^n . With the approximation that the problem is separable in the coordinate r and all the s_n, the addition of other vibrational modes just leads to other factors similar to 41.

Schwartz, Slawsky and Herzfeld have adapted these results to practical

problems by employing a more realistic potential than 35. An emperical potential which has been useful in many problems involving the interaction of gas molecules is the Lennard - Jones (6-12) potential

$$H = -4\epsilon\left[\left(\frac{\sigma}{r}\right)^6 - \left(\frac{\sigma}{r}\right)^{12}\right] \tag{42}$$

ϵ is the depth of the attractive portion of the potential, and σ is the distance of approach at which H = 0. The parameters, ϵ and σ, have been obtained for many gases by emperical fit from viscosity data and second virial coefficients by Hirschfelder (10).

Unfortunately one cannot solve equation 34 in closed form for the Lennard - Jones potential. Since only the relatively high velocity collisions are important for energy transfer, S-S-H have assumed that just the repulsive part of 42 need be considered. They have matched the repulsive portion of the Lennard - Jones potential and the exponential potential 35 by equating H and $\frac{d\,H}{d\,r}$ at the point r_1 which is arbitrarily taken as the classical distance of closest approach of the two molecules with relative velocity v. They have shown (1) that for potentials whose value of ϵ is not too great the approximation

$$\alpha^* = \frac{17.5}{r} \tag{43}$$

is valid. By the use of this relation the results obtained with the mathematically tractable exponential potential can be converted into calculations utilizing the Lennard - Jones parameters.

Schwartz and Herzfeld (11) have extented the calculation to three dimensions and considered the effect of the attractive portion of the

potential. The results are essentially the same as for the one dimensional treatment. The effective collisions are again found to be those of high relative velocity. The effect of the centrifugal energy and the attractive portion of the potential is to modify the relative velocity. The centrifugal term decreases the relative velocity; the attraction increases the velocity. Both effects are relatively minor in the overall probability of energy exchange.

$P^{i,\,i+1}$ can be calculated from 28 by substitution of the various factors which determine a_j. The probability thus determined is an explicit function of the velocity. It is necessary to average expression 28 over a suitable Boltzman distribution of velocities to arrive at the final probability of energy exchange per average collision.

The final, working expressions for the probability of vibrational energy exchange are given below for the three cases of interest in this investigation - non-resonant, near-resonant, and exact-resonant transitions. These expressions are based on the three-dimensional theory of Schwartz and Herzfeld (11).

(a) Non-resonant probability: the diatomic molecule B is deactivated from the first vibrational level to the ground state, and this energy is put into relative translational motion of the collision pair.

$$P^{10}_{(B,A)} = P_o V^2_{(B)_{10}} \left\{ 8\left(\frac{\pi}{3}\right)^{1/2} \left(\frac{8\pi^3 \mu \Delta E}{\alpha^{*2} h^2}\right)^2 \chi^{1/2} e^{-3\chi + \frac{\Delta E}{2kT} + \frac{\epsilon}{kT}} \right\} \tag{44}$$

where

$$\chi = \left[\frac{2\pi^4 \mu (\Delta E)^2}{\alpha^{*2} h^2 kT}\right]^{1/3}$$

$$\Delta E = h\nu_B \tag{45}$$

$$V^2_{(B)_{10}} = \frac{\alpha^{*2} h}{32\pi^2 \nu_B \mu_B}$$

P_o is a steric factor to correct for orientation of the collision. All the other quantities are as previously defined.

(b) Near-resonant probability: the molecule B is deactivated while molecule A is activated. However, there is still sufficient energy exchange with the translational motion so that relation 39 is applicable.

$$P^{10}_{01(B,A)} = V^{2}_{01(A)} \; P^{10}_{(B,A)} \tag{46}$$

where

$$V^{2}_{01(A)} = \frac{\alpha^{*2} h}{32 \pi^2 \nu_A \mu_A}$$

$$\Delta E = h\nu_B - h\nu_A \tag{47}$$

(c) Exact-resonancy probability: vibrational energy is exchanged between the molecules, but no energy is exchanged with translation. Therefore, relation 40 can be used

$$P^{10}_{01(B,A)} = P_o V^{2}_{10(B)} V^{2}_{01(A)} \frac{64 \pi \mu k T}{\alpha^{*2} h^2} e^{\epsilon/kT} \tag{48}$$

Calculations

Equations 23 and 24 were solved simultaneously for the physical situation A = O_2 and B = N_2. The equations were integrated numerically on an ElectroData Datatron computer, Model 205, employing a modified Kutta fourth order method. Some details of this integration procedure are described in Appendix I.

The vibrational transition probabilities were calculated from formulae 44 - 47. The molecular parameters needed for these calculations are shown in Table I.

Table I

Molecular Parameters for Calculating P's

		O_2	N_2	Source
σ	(A)	3.50	3.715	(10)
ϵ/k	(°K)	100	85.7	(10)
ν (1→O)	(cm^{-1})	1556	2332	(12)

In Table 2 the various transition probabilities and other quantities needed for a numerical solution of equations 23 and 24 are listed for the range of temperatures considered in this problem.

Table 2

Vibrational Transition Probabilities

$A \equiv O_2$, $B \equiv N_2$

T °K	$P^{10}_{(A,M)}$	$P^{10}_{(B,M)}$	$P^{10}_{(A,B)}_{o\ 1}$	$P^{10}_{(B,A)}$	$Z_{x10^{-9}}$	$1-e^{-\alpha}$	$1-e^{-\beta}$
1000	7.50×10^{-6}	4.25×10^{-8}	3.50×10^{-6}	1.00×10^{-5}	3.60	0.893	0.965
2000	2.50×10^{-4}	4.00×10^{-6}	5.70×10^{-5}	1.00×10^{-4}	2.50	0.674	0.813
3000	1.50×10^{-3}	4.25×10^{-5}	2.00×10^{-4}	3.00×10^{-4}	2.00	0.526	0.673
4000	5.00×10^{-3}	2.00×10^{-4}	4.70×10^{-4}	6.20×10^{-4}	1.80	0.429	0.568
5000	1.00×10^{-2}	5.75×10^{-4}	8.30×10^{-4}	1.00×10^{-3}	1.60	0.361	0.489
8000	5.50×10^{-2}	4.00×10^{-3}	2.40×10^{-3}	2.75×10^{-3}	1.25	0.244	0.324

The non-resonant probability, $P^{10}_{(A,M)}$, was calculated by taking the approximate average of $P^{10}_{(A,A)}$ and $P^{10}_{(A,B)}$ and similarly for $P^{10}_{(B,M)}$. For oxygen and nitrogen $P^{10}_{(A,A)}$ and $P^{10}_{(A,B)}$ differ at the most by 5% as calculated from equation 44, and the use of the effective molecule, M, in deriving the macroscopic relaxation equations is justified. To calculate the probabilities which involve A-B collisions the Lennard - Jones parameters in Table I must be modified by using the emperical combining rules (13)

$$\sigma_{A,B} = \tfrac{1}{2}\left(\sigma_A + \sigma_B\right)$$
$$\left(\epsilon/k\right)_{A,B} = \sqrt{\left(\epsilon/k\right)_A \left(\epsilon/k\right)_B} \qquad (49)$$

The macroscopic relaxation equations can be further simplified if it is assumed that an average collision frequency, Z, can be used, i.e.,

$$Z_{A,M} \approx Z_{B,M} \approx Z_{A,B} \approx Z_{B,A} = Z \qquad (50)$$

This is the Z listed in Table 2, and it is calculated for a total pressure of one atmosphere at the indicated temperature.

The particular values of temperature shown in Table 2 were chosen to include a wide range of non-resonant to near-resonant probabilities. This is indicated in Table 3.

Table 3

Range of Transition Probabilities

T °K	$P^{10}_{01}(A,B) / P^{10}(A,M)$	$P^{10}_{01}(B,A) / P^{10}(B,M)$
1000	.47	235
2000	.23	25
3000	.13	7.1
4000	.094	3.1
5000	.083	1.7
8000	.044	0.69

The calculation was performed at each of the six temperatures shown in Table 2 for the pure gases and for the following four mixtures:

a	b
0.01	0.99
0.10	0.90
0.20	0.80
0.50	0.50

The thermodynamic internal energy functions for oxygen and nitrogen have been tabulated for the temperatures of interest in Table 4.

Table 4

Internal Energy Function, $\frac{E^\circ - E_o^\circ}{RT}$

T	Oxygen				Nitrogen			
°K	Total	Vib.	Elect.	Correc.	Total	Vib.	Elect.	Correction
298.16	2.493	0.004	-	-	2.498	0.0002	-	-
500	2.547	0.052	-	-	2.508	0.008	-	-
1000	2.775	0.267	8.6×10^{-5}	0.008	2.624	0.122	-	0.002
2000	3.082	0.543	0.013	0.026	2.898	0.386	-	0.012
3000	3.281	0.673	0.060	0.048	3.066	0.543	-	0.023
4000	3.439	0.746	0.119	0.074	3.172	0.693	-	0.033
5000	3.567	0.793	0.171	0.103	3.246	0.702	2.7×10^{-5}	0.044
8000	3.796	0.867	0.262	0.167	3.380	0.805	0.005	0.077

The values of the total internal energy are taken from the tabulations in the NBS, Series III (14) and from high temperature calculations on air by Gilmore (15). The vibrational contribution to the energy was calculated using the harmonic oscillator approximation tabulated by Pitzer (16). The electronic contribution to the internal energy was obtained assuming a complete separation of the electronic partition function. At these temperatures the electronic energy is only important for oxygen.

The column headed "correction" in Table 4 was calculated by subtracting from the total energy the contributions due to translation and rotation (2.50), the harmonic oscillator energy, and the electronic energy. Therefore, this number is a measure of the extent to which the vibrational energy is influenced by anharmonicity and interaction with rotation. For oxygen it

also includes any correction caused by the variation of vibrational constants in the excited electronic states. For the calculations of the quantities in Table 4 all the necessary physical data were obtained from Herzberg (12).

In the integration of the macroscopic relaxation equations oxygen and nitrogen were assumed to be initially (t = 0) vibrationally cold, i. e.,

$$E_A/\bar{E}_A = E_B/\bar{E}_B = 0 \tag{51}$$

As one can see from Table 4, this is approximately the situation at room temperature. The calculations presented here correspond to the sudden, instantaneous heating of mixtures of oxygen and nitrogen from about room temperature up to the final equilibrium temperature at a total pressure of one atmosphere. Such a physical situation could be obtained by shock wave heating.

Results

Data. The results of these calculations are shown in Figures 1 - 6. Each figure summarizes the results for a particular temperature and the various concentrations. The oxygen relaxation is described by the five small graphs on the left side of the figures; the nitrogen relaxation is on the right. Each small graph is a plot of the fraction of equilibrium vibrational energy versus time and approaches 1.00 asymptotically. In each figure the top pair of graphs shows the relaxation behavior of the pure gases at that temperature, and each successive pair of graphs shows the relaxation of the components of a particular mixture. The numerical data from which these graphs were constructed are listed in Appendix 2 in Tables 11 - 16.

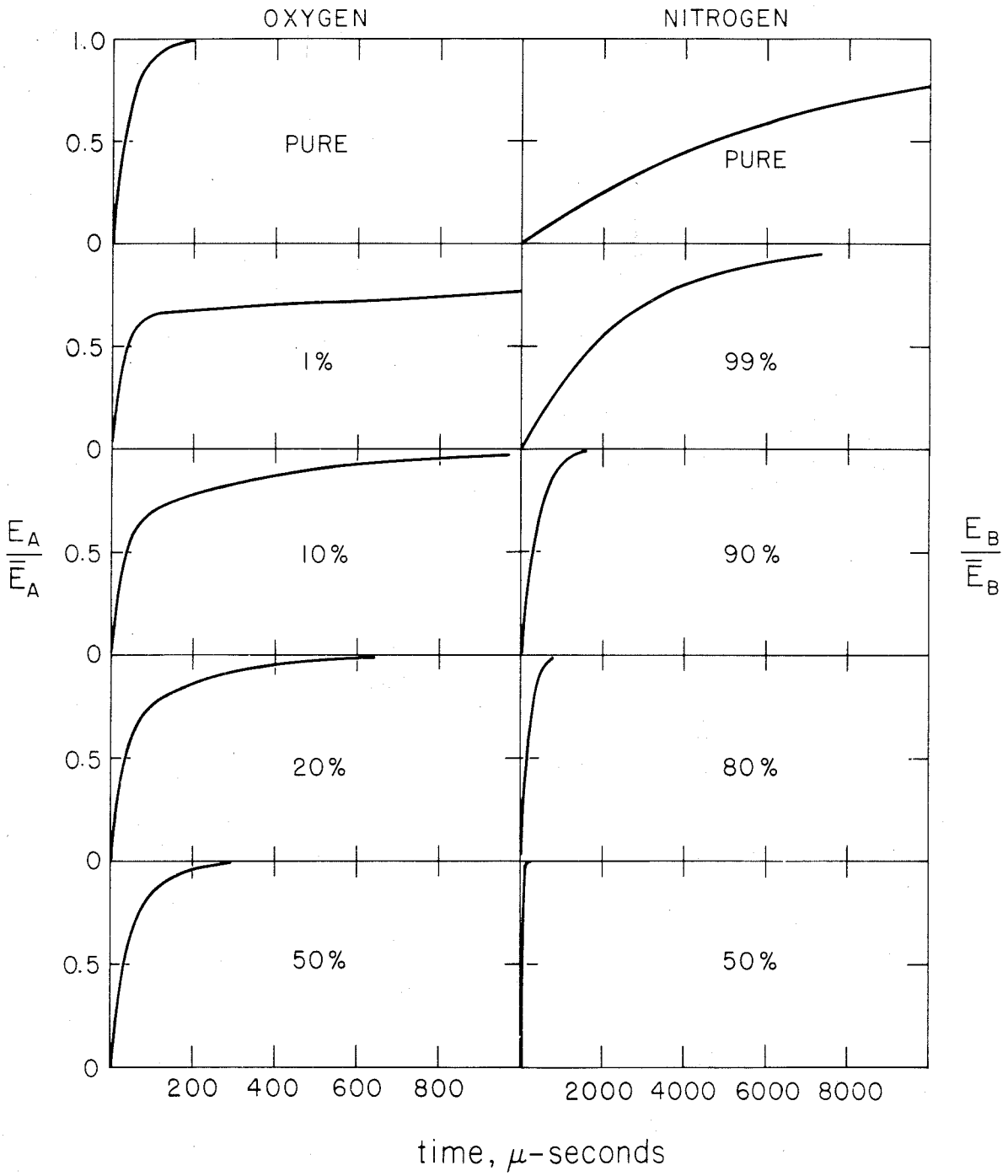

FIG. 1 – VIBRATIONAL RELAXATION AT 1000° k

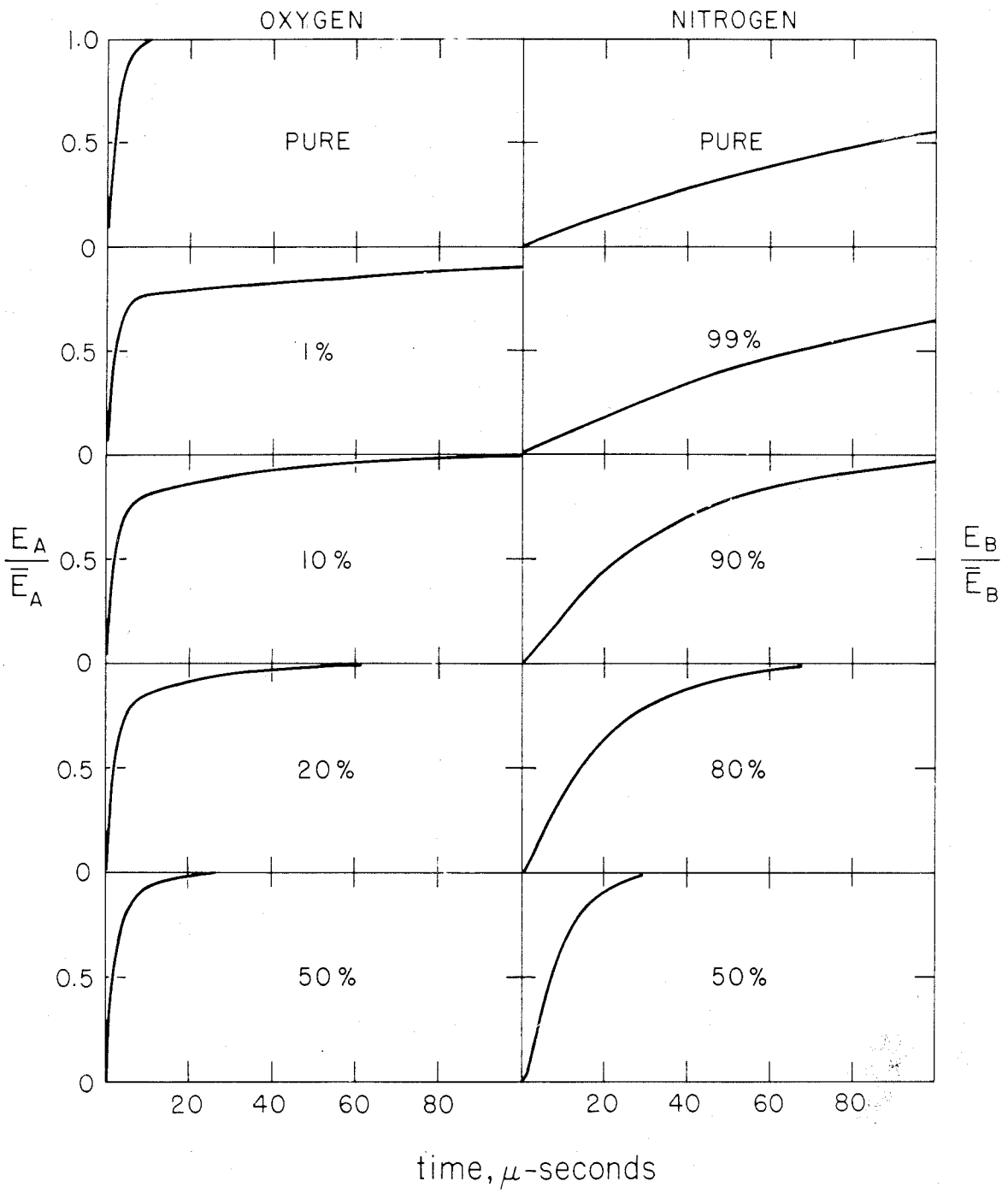

FIG. 2 – VIBRATIONAL RELAXATION AT 2000° k

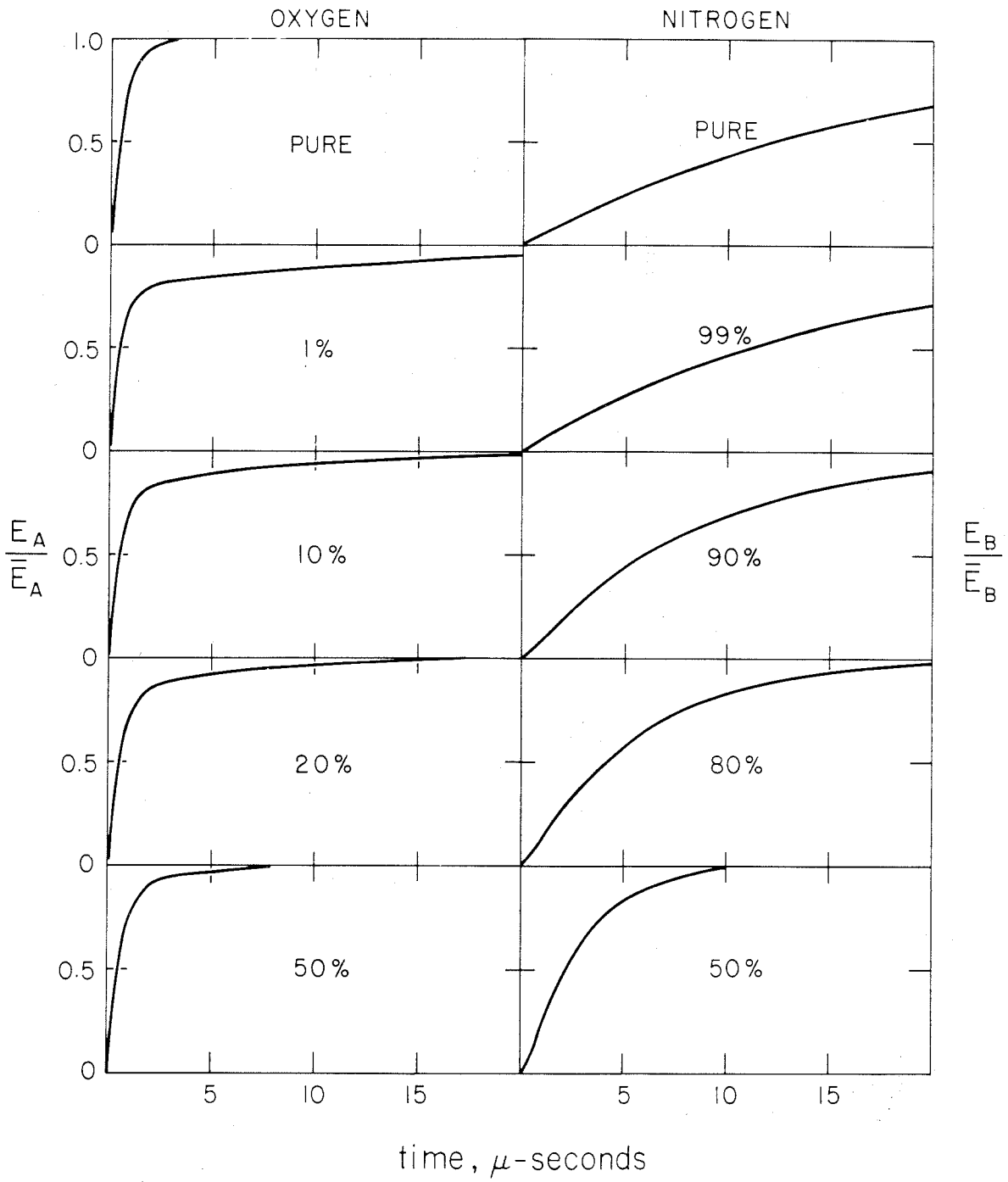

FIG. 3 – VIBRATIONAL RELAXATION AT 3000° k

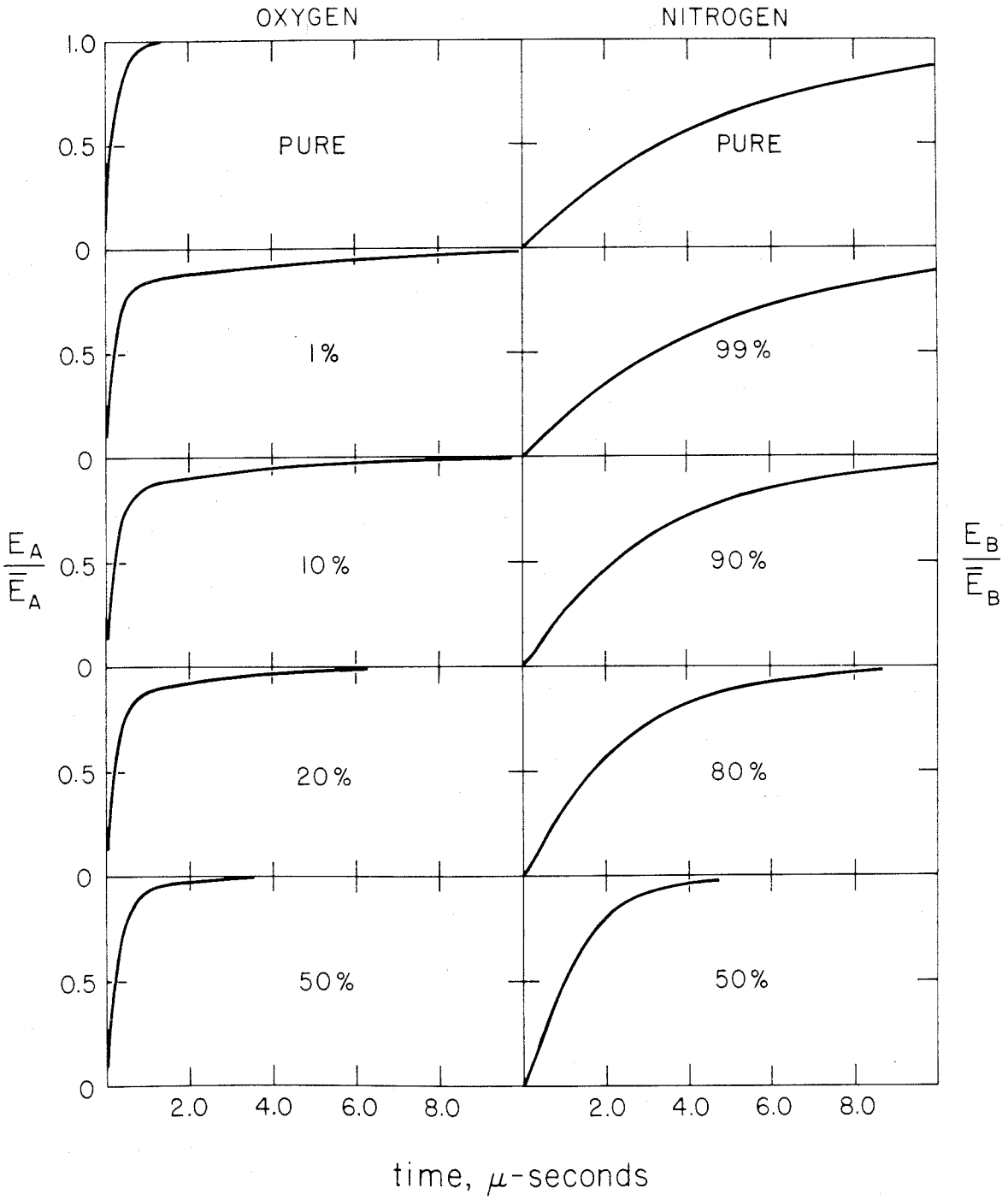

FIG. 4- VIBRATIONAL RELAXATION AT 4000° k

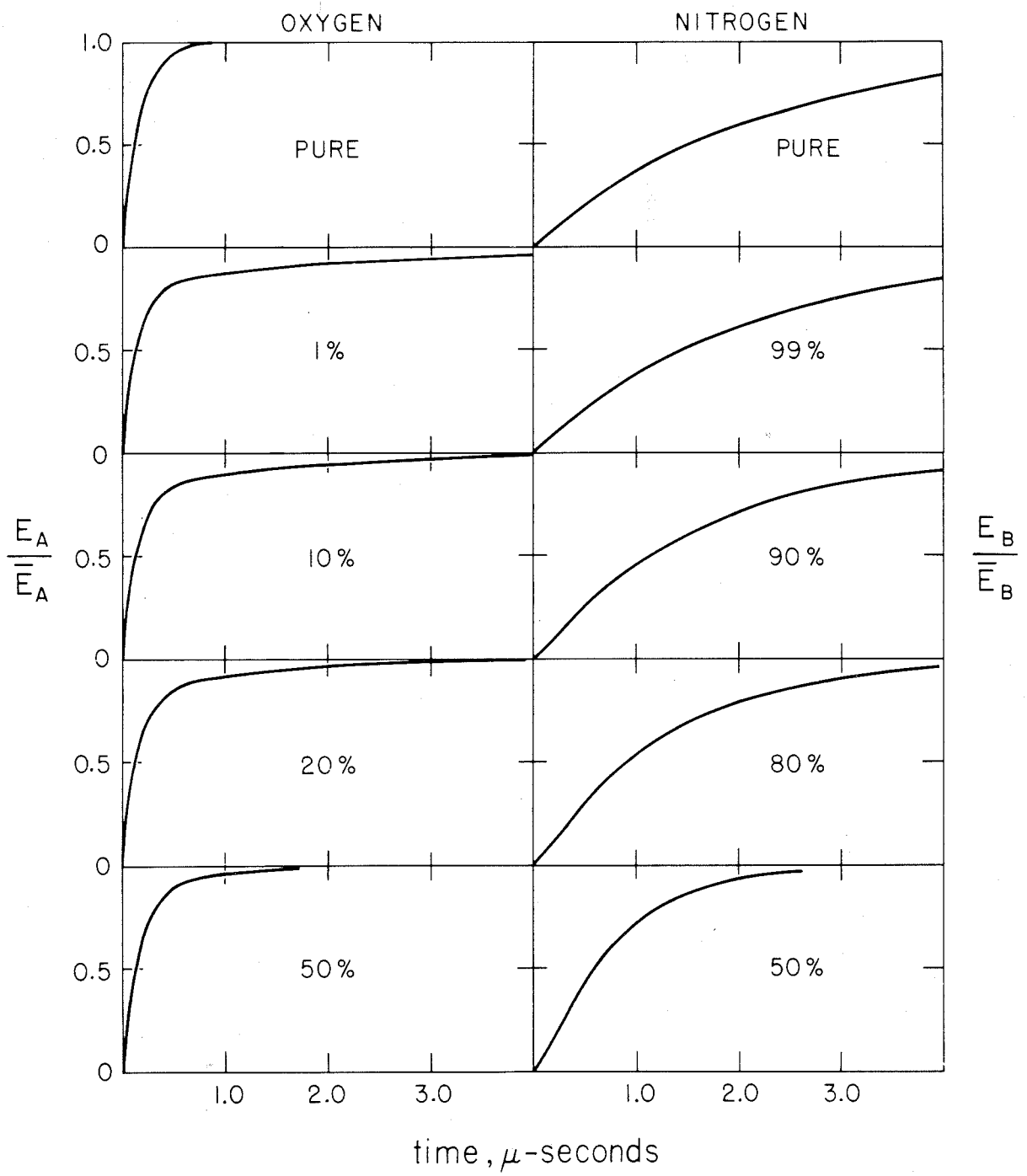

FIG. 5–VIBRATIONAL RELAXATION AT 5000° k

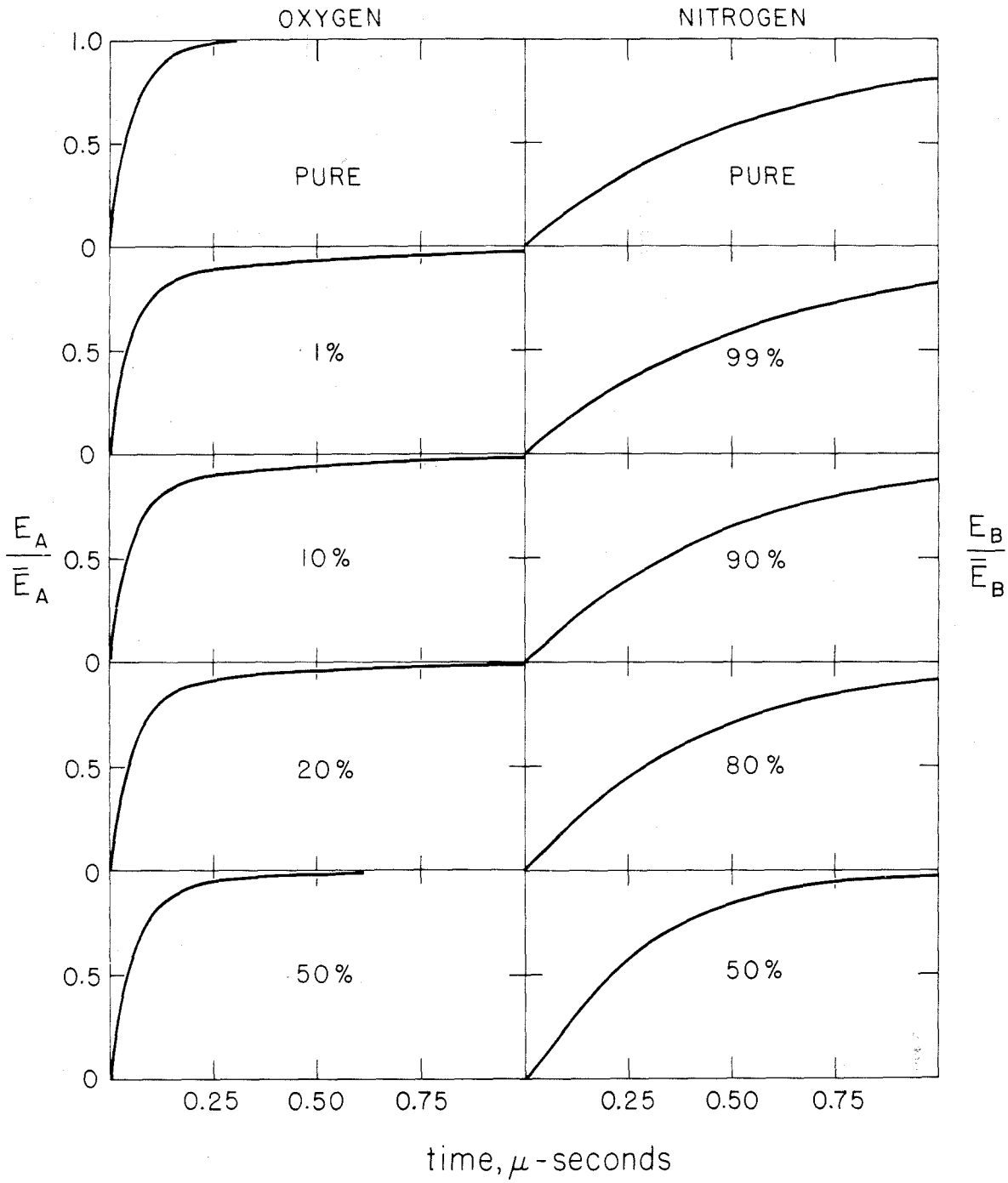

FIG. 6 – VIBRATIONAL RELAXATION AT 8000° K.

Interpretation of Results. It is obvious from an inspection of Figure 1 - 6 that, using the theoretical values of the excitation probabilities, the inclusion of a near-resonant mechanism for energy exchange has a significant effect on the vibrational relaxation of nitrogen. This is particularly noticeable at the lower temperatures where the near-resonant probability for nitrogen is orders of magnitude greater than the non-resonant probability (see Table 3).

This result can be interpreted physically as follows: The relaxation of pure oxygen is much faster than that of pure nitrogen. As soon as there is an appreciable concentration of vibrationally excited oxygen molecules, energy begins to be transferred into the vibrational mode of nitrogen by near-resonant collisions. If the probability of this latter process is much greater than the direct excitation of nitrogen, the rate of relaxation of nitrogen will follow the rate of the resonant mechanism.

The removal of vibrational energy from oxygen by nitrogen is expected to affect the relaxation behavior of the oxygen. Inspection of Figure I, for example, shows that the time for the oxygen to attain 0.6 - 0.7 of its equilibrium vibrational energy is approximately the same in the mixtures as in the pure gas. However, the final stages of the relaxation occur more slowly in the mixtures. This effect is most noticeable for the case of 1% oxygen. In the more concentrated mixtures the excitation of the oxygen is able to keep pace with the resonant process.

The near-resonant probability of energy exchange has a weaker temperature dependence than the non-resonant probability.* Therefore, as the temperature increases the importance of the near-resonant process to the non-resonant

---

* This is due to the smaller term, χ , in the exponential which is the primary source of temperature dependence in the expression for the probability. Compare expressions 45 and 47.

decreases. At 8000° K the resonant mechanism has only a small effect on the vibrational relaxation of nitrogen.

The results of this investigation demonstrate that the effect of a resonant process in a mixture of two gases is most noticeable if the two gases have a large difference in their pure, non-resonant relaxation times. The primary result of the resonant process is to increase the relaxation of the slower component.

Schwartz, Slawsky and Herzfeld in their analysis of the vibrational relaxation of gas mixtures concluded that the system N_2 - CO should be an example of a mixture that would exhibit a resonance effect and, therefore, would have a short relaxation time. The fundamental vibration frequencies of nitrogen and carbon monoxide are nearly equal (N_2: ω_e = 2360 cm^{-1}, CO: ω_e = 2170 cm^{-1}), and the resonance exchange of energy is expected to be very efficient. However, as is shown in Appendix 1 to Part I of this thesis the pure gases have approximately the same relaxation times. Even though the molecules can exchange energy with each other relatively easily, the rate of formation of vibrational energy in the mixture will be limited by the non-resonant excitation rates which are essentially identical. On the basis of the present investigation no large effect on the relaxation time of the system N_2 - CO due to a resonance exchange of energy is predicted.

Approximate Treatment. The physical interpretation just described can be used as a basis for an approximate analysis of the vibrational relaxation of this two component system. The assumption is made that the oxygen is

completely relaxed in a time short compared to the nitrogen relaxation. This is equivalent to setting $E_A/\bar{E}_A = 1$ in equation 24 which then becomes

$$\frac{d(E_B/\bar{E}_B)}{dt} = Z\left\{P(B,M)^{10}(1-e^{-\beta}) + a\,P(B,A)^{10}_{01}\left(\frac{1-e^{-\beta}}{1-e^{-\alpha}}\right) - \left[P(B,M)^{10}(1-e^{-\beta}) + a\,P(B,A)^{10}_{01}\left(\frac{1-e^{-\alpha}}{1-e^{-\beta}}\right)\right]\right\} E_B/\bar{E}_B \tag{52}$$

This equation is easily integrated and with the initial condition 51 yields

$$E_B/\bar{E}_B = 1 - e^{-t/\tau_M} \tag{53}$$

where the relaxation time, τ_M, for nitrogen in the mixture is defined as

$$1/\tau_M = Z\left[P(B,M)^{10}(1-e^{-\beta}) + a\,P(B,A)^{10}_{01}\left(\frac{1-e^{-\beta}}{1-e^{-\alpha}}\right)\right] \tag{54}$$

The relaxation time for a pure nitrogen, τ_B, is defined as

$$1/\tau_B = Z\,P(B,M)^{10}(1-e^{-\beta}) \tag{55}$$

If τ_R defined as

$$1/\tau_R = Z\,a\,P(B,A)^{10}_{01}\left(\frac{1-e^{-\beta}}{1-e^{-\alpha}}\right) \tag{56}$$

is called the relaxation time for the near-resonant process, then 54 can be rewritten

$$\frac{1}{\tau_M} = \frac{1}{\tau_B} + \frac{1}{\tau_R} \tag{57}$$

or

$$\tau_M = \frac{\tau_B\,\tau_R}{\tau_B + \tau_R} \tag{58}$$

In this approximation the relaxation time of the nitrogen in the mixture is given by the reduced relaxation times of the non-resonant and near-resonant processes.

To compare the approximate treatment with the exact results obtained by numerical integration of the relaxation equations, it will be convenient to define a quantity

$$X = \tau_M / \tau_B \tag{59}$$

In terms of relation 58 X can be expressed as

$$X = \frac{1}{1 + \tau_B / \tau_R} \tag{60}$$

Therefore, the quantity of significance for this comparison is

$$\frac{\tau_B}{\tau_R} = \frac{a \, P^{10}_{01(B,A)}}{(1 - e^{-\alpha}) \, P^{10}_{(B,M)}} \tag{61}$$

The results of this comparison are presented in Table 5 for three temperatures- 1000°, 2000° and 5000°K.

Table 5

Comparison of Approximate and Exact Calculations

T °K	a	τ_B/τ_R	X Approx.	X Exact	$X_{ex.}/X_{app.}$	$\tau_M^{(B)}/\tau_M^{(A)}$	$\tau_M^{(B)}/\tau_M^{(A)}$
1000	Pure	-	-	-	-	160	69
	0.01	2.64	0.275	0.37	1.35	30	0.83
	0.10	26.4	0.037	0.059	1.62	5.8	0.82
	0.20	52.8	0.019	0.034	1.79	3.8	0.87
	0.50	132	0.0075	0.016	2.04	2.2	0.73
2000	Pure	-	-	-	-	49	22
	0.01	0.371	0.73	0.80	1.10	28	0.98
	0.10	3.71	0.21	0.28	1.33	11	1.1
	0.20	7.42	0.12	0.16	1.33	6.7	1.1
	0.50	18.6	0.051	0.080	1.57	3.5	1.2
5000	Pure	-	-	-	-	13	5.6
	0.01	0.048	0.955	0.946	0.99	11	1.4
	0.10	0.482	0.675	0.73	1.08	7.9	1.4
	0.20	0.964	0.51	0.57	1.12	6.5	1.6
	0.50	2.41	0.29	0.36	1.24	4.5	1.6

The relaxation times for the mixtures were arbitrarily defined as the time for the energy to reach 1 - $1/e$ or 0.632 of its equilibrium value, even though these relaxation curves are not expected to be true exponentials. The sixth column of Table 5 shows that the approximate method predicts the

change in the relaxation time of nitrogen in the mixtures to within a factor of two in every case.

The last two columns of Table 5 illustrate the extent to which the assumption used in this treatment is valid. $\tau_M'^{(A)}$ is defined as the time for the oxygen to relax to 9/10 of its equilibrium value. If the oxygen is relaxed in a time short compared to the nitrogen then the ratios $\tau_M^{(B)}/\tau_M^{(A)}$ and $\tau_M^{(B)}/\tau_M'^{(A)}$ should be larger than one. The trend of these ratios is seen to be consistent with the observation that the accuracy of this method decreases as the fraction of oxygen increases. But there does not seem to be any clear relation between the accuracy of the method and the extent to which the oxygen must be completely relaxed.

The relative insensitivity of the method to the validity of the approximation is a consequence of the form of the relaxation equation. When resonant or near-resonant exchange is important, $\alpha \approx \beta$, and the nonlinear term in this equation will be small because of the factor $e^{-\alpha} - e^{-\beta}$. Therefore, linearization of this equation by setting $E_A = \bar{E}_A$ does not have a large influence even if the approximation is poor.

Comparisons with Experiment

Oxygen - Nitrogen System. There is insufficient evidence to date to check the validity of using the S-S-H theory to estimate the probabilities of near-resonant and resonant energy exchange processes in vibrational relaxation. However, the non-resonant probabilities for oxygen and nitrogen are reasonably well predicted by the theory. This point is illustrated in Figure 6 of Part I of this thesis. The theoretical values of relaxation times for oxygen and nitrogen shown in this graph are based on the same non-resonant probabilities that were used in the present work. It is evident that there is agreement with experimental values to within a factor of about two or three over the temperature range of 1000° - 5000°K. The justification of the present calculation is based on this obvious usefulness of the S-S-H theory for predicting the non-resonant relaxation behavior of oxygen and nitrogen. The validity of using the theory for near-resonant processes can only be tested by comparison with experimental data on gas mixtures.

The vibrational relaxation of air and oxygen - nitrogen mixtures has been measured by a sound absorption technique at room temperature by Kneser and Knudsen (17). They found that O_2 - N_2 collisions were about five times more efficient in relaxing oxygen as O_2 - O_2 collisions. This result cannot be explained by the near-resonant exchange of vibrational energy, since the major effect of the near-resonant process is expected to be on the relaxation time of nitrogen. At room temperature the equilibrium constant of the reaction

$$O_2^*(v=1) + N_2(v=0) \rightleftharpoons O_2(v=0) + N_2^*(v=1) \qquad (62)$$

is calculated from the Boltzman factor to be 0.024. The equilibrium of the resonant exchange reaction lies far to the left, and its influence on the vibrational relaxation of the mixture is negligible.

Blackman (18) has studied the vibrational relaxation of a series of oxygen - nitrogen mixtures (20 - 66% O_2) at temperatures of 1700 - 2400°K. These experiments were performed in a shock tube. The relaxation behavior was studied by following the density change behind the shock with an interferometer. As the gas relaxes, its translational temperature decreases, and its density increases. Blackman assumed that the nitrogen was completely unrelaxed during the experiment. This will not be true if the near-resonant mechanism is operative. With the assumption of unrelaxed nitrogen Blackman calculated that the O_2 - N_2 collisions were about 40% as effective in relaxing the oxygen as O_2 - O_2 collisions.

The final equilibrium densities of the shocked gas measured by Blackman agree reasonably well with the values expected assuming the nitrogen unrelaxed. If the near-resonant mechanism exists, the nitrogen should relax quickly, and this fact should be reflected in the final equilibrium density of the gas. The point is illustrated in Figure 7, where the total vibrational energy of air* has been plotted as a function of time for four temperatures. Two cases are shown. The dashed line represents the relaxation behavior of air if there is no resonant process and the gases have their pure relaxation times, and the full line is based on the present calculations including the resonant mechanism. The equilibrium energy of air, $\overline{E}_{Air}$, and the contribution of oxygen, $\overline{E}_{O_2}$, are indicated by the horizontal lines.

At the lower temperatures with the assumption of no resonance the vibrational energy of air is seen to relax in two steps. The oxygen component relaxes rapidly, and then, the slower equilibration of the nitrogen takes place. With the inclusion of the near-resonant mechanism the relaxation of the total vibrational energy of air takes place much more rapidly, and only one relaxation curve is apparent.

Based on Figure 7 at 2000° the vibrational relaxation time for air with a resonant process is about 20 μsec. Blackman at about this same temperature obtained a value of about 1-2 μsec at a total pressure of 1 atmosphere. As can be seen from Figure 7 for the case of no resonance, the vibrational energy of oxygen will equilibrate rapidly (5-7 μsec), and, then, the remaining equilibration of the nitrogen vibrational energy will take place over several hundred micro-seconds. It is doubtful is this long relaxation time for nitrogen would be resolved in Blackman's experiment. Therefore his experiments are best described by the non-resonant behavior of air with only the relaxation of the oxygen being observed.

The method employed by Blackman determines the relaxation times by the deviation from horizontal alignment of a set of interference fringes.

---

* The vibrational energy of air was calculated from the harmonic oscillator energies listed in Table 4 assuming a mixture of 20% O_2 and 80% N_2.

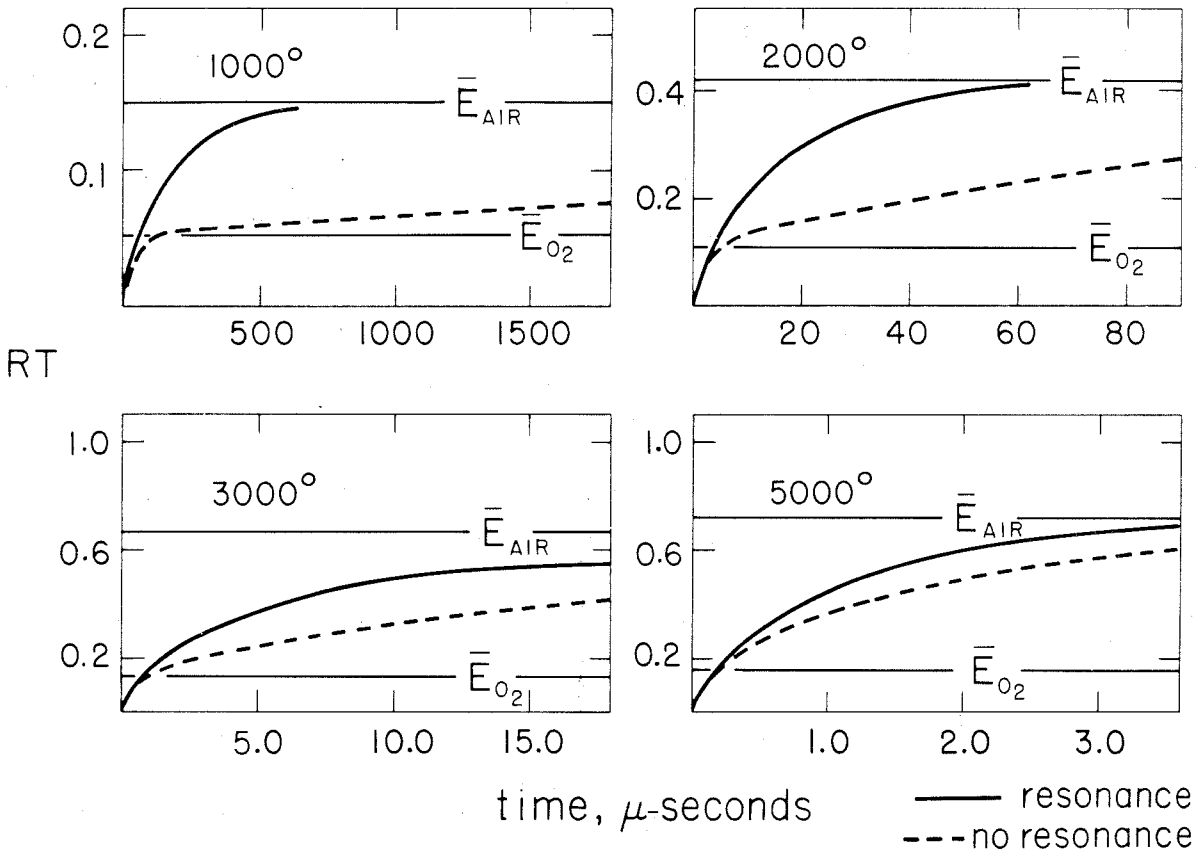

FIG. 7— RELAXATION OF VIBRATIONAL ENERGY OF AIR.

Blackman has included a set of typical interferograms in his paper, and it does not seem possible to reinterpret these in terms of the large resonant effect predicted by the present investigation. However, a smaller resonant effect, e.g., a half or third of the resonant probability assumed in the present calculation, might go undetected in Blackman's experiment.

Resonant Exchange in Polyatomic Gases. At present the polyatomic gases offer the best experimental evidence of the existence of resonant energy transfer in vibrational relaxation. In a polyatomic molecule the excitation of a high frequency vibrational mode may be more probable by means of resonant or near-resonant transfer with a low frequency mode than by direct excitation from translation. The situation is entirely analogous to the present discussion of mixed gases, and similar relaxation equations for the various modes of the molecule can be derived (1, 3). In polyatomic gases resonance probabilities describing transitions of more than one quantum per mode per collision are often important, and the derivation of the macroscopic relaxation equation is somewhat more complicated.

Tanczos (3) has compared the relaxation behavior of the chloromethanes based on theoretical transition probabilities calculated by the S-S-H theory with the experimental results. For methylene chloride two distinct relaxation times are predicted. Two sound dispersion regions have been found in ultrasonic measurements by Sette, Busala, and Hubbard (19). The comparison of the theoretical and experimental values of relaxation times is given in Table 6.

Table 6

Comparison of Relaxation Times in Methylene Chloride

	τ_1 μsec		τ_2 μsec	
^oK	Experiment	Theory	Experiment	Theory
303	0.0015	0.012	0.070	1.3

τ_1 represents the relaxation time associated with the non-resonant deactivation of the lowest mode - $P^{10}_{(1)}$ *. τ_2 is the relaxation time associated with the near-resonant deactivation of the second mode together with a two quantum activation of the first mode - $P^{10}_{(2,1)}$ *. The frequencies of the lowest four vibrational modes of CH_2Cl_2 are 283, 704, 737, and 899 cm^{-1} (19). For the third and higher modes resonant transitions with the second mode are sufficiently fast so that the rate of excitation of the second mode is the rate determining step and, therefore, only two distinct relaxation times are found.

The situation for the other chloromethanes is not so clear. The calculations for CH_3Cl, $CHCl_3$, and CCl_4 indicate that these gases should exhibit multiple relaxation times, but experiments to date do not substantiate this prediction.

Sulfur dioxide is another polyatomic gas which has been found experimentally (20) to have two relaxation times. The vibration frequencies of the molecule are (21) ν_1 - 519 cm^{-1}, ν_2 -1151 cm^{-1},

* These symbols for transition probabilities are similar to those defined previously. The numbers 1, 2, etc., within the parenthesis refer to the vibrational mode(s) undergoing the transition.

ν_3 - 1361 cm^{-1} .* Dickens and Linnett (22) have calculated the various resonant and non-resonant rates of excitation of this molecule using the S-S-H theory. Their results are reproduced in Table 7.

Table 7

Calculated Values of Transition Rate Constants and Comparison of Relaxation Times in SO_2

T	$K^{10}_{(1)}$	$K^{10}_{(2,1)}$ 02	$K^{10}_{(3,2)}$ 01	$K^{10}_{(2)}$	τ_1		τ_3	
°K	x10^{-5} sec^{-1}	x10^{-5} s^{-1}	x10^{-5} s^{-1}	x10^{-5} s^{-1}	μsec		μsec	
373	27.8	10.4	16.4	0.002	0.071	0.29	0.82	1.5

The rates of other possible transitions not shown in Table 7, e.g., for the process $K^{10}_{(3)}$, are much smaller than the values of the transitions listed and are not important mechanisms for vibrational equilibration of SO_2.

Using these rate constants in the relaxation expression for the sound velocity Dickens and Linnett have been able to reproduce the two regions of sound dispersion found experimentally. The shorter relaxation time τ_1, corresponds to non-resonant deactivation of the lowest mode, $K^{10}_{(1)}$, while the longer relaxation time, τ_3, corresponds to the near-resonant exchange of energy between the second and third modes, $K^{10}_{(3,2)}$. These processes are calculated to have the fastest rates.
01

The results in Table 7 show that the calculated relaxation times are about a factor of two to five times larger than the experimental values.

* The numbering of the modes follows the convention of Dickens and Linnett.

Therefore, the theoretical transition probabilities are smaller than the experimental probabilities by a like factor. The comparison of the data for the methylene chloride in Table 6 shows a similar trend although the discrepancy between the experimental and calculated values is somewhat larger.

For the gases SO_2 and CH_2Cl_2 the experimental evidence indicates that the upper-vibrational modes relax principally by a near-resonant exchange with a lower mode. The agreement between the resonant probabilities calculated by the S-S-H theory and experimentally derived values is within an order of magnitude.

Effect of H_2O on Vibrational Relaxation. Water has a very large effect on the vibrational relaxation of some substances. In many gases only traces of water vapor decrease the relaxation time by several orders of magnitude. For the particular example of H_2O in CO_2 strong chemical forces besides the usual Van der Waals forces between molecules have been suggested to explain this phenomenon (23). Water has also been found to have a large effect in O_2, N_2, and CO. The occurrence of strong "chemical interactions" in these systems is doubtful.

The fundamental vibrational frequencies of the water molecule are (24): ν_1 - 3652 cm^{-1}, ν_2 - 1595 cm^{-1}, ν_3 - 3756 cm^{-1}. Except at high temperatures only the bending mode ν_2 is important. It is evident that the magnitude of the frequency of ν_2 is convenient for H_2O to engage in near-resonant energy exchange with N_2 and CO and almost exact resonance with O_2. The vibrational relaxation time of pure H_2O has been measured by Huber and Kantrowitz (25) and found to be 2-4 x 10^{-8} sec in the temperature range of 500 - 700°K. This is many orders of magnitude

faster than for O_2, N_2, or CO at the same temperature.

Water has the two requirements necessary for it to act as a "resonant impurity." It has a vibrational frequency of the right magnitude to engage in resonant or near-resonant energy exchange, and it has a fast relaxation time relative to the principal gas. The relaxation time of pure H_2O is so fast compared to O_2, N_2, or CO that the use of the approximate method outlined previously is justified. If the relaxation times of the pure gas and for mixtures with the mole fraction, a, of water vapor are known, then the use of relations 59, 60, and 61 allows the calculation of the resonant or near-resonant probability - $P^{10}_{01}(B, H_2O)$.

H. and L. Knötzel (26) have measured the effect of H_2O on the relaxation time of O_2 at 19°C by a resonance sound absorption technique. They obtained an equation of the form

$$f_{max} = 0.040 + 195\ a + 1.32 \times 10^6\ a^2 \qquad (63)$$

for the frequency of maximum absorption, f_{max}, in kilocycles per second as a function of the concentration, a, of added H_2O. The relation between relaxation time, τ, and f_{max} is

$$\tau = \frac{1}{2\ \pi\ f_{max} \times 10^3} \qquad (64)$$

The quadratic concentration dependence of equation 63 is interpreted by the authors as due to the large effect of three body collisions of one O_2 and two H_2O molecules on the vibrational relaxation of this system. Using the experimental data of H. and L. Knötzel for pure oxygen and only the linear term of equation 63 the resonant probability $P^{10}_{01}(O_2, H_2O) = 2.0 \times 10^{-4}$ is obtained. For comparison the probability calculated

from the exact resonance form of the S-S-H theory (equation 48) is 43×10^{-4}. To obtain the effective Lennard - Jones parameters, σ and ϵ, for the O_2-H_2O collision the combining rules for a polar, non-polar interaction (27) were used. The values of σ and ϵ for the pure gases and the values calculated from the combining rules are listed in Table 8.

Table 8

Lennard - Jones Parameters (10)

Interaction	σ $\mathring{A}$	ϵ/k ^{o}K
H_2O - H_2O	2.65	380
O_2 - O_2	3.46	118
O_2 - H_2O	3.03	237
N_2 - N_2	3.70	95
N_2 - H_2O	3.14	213
CO - CO	3.76	100
CO - H_2O	3.18	218

It is seen that the experimental and theoretical values of differ by a factor of 20. Perhaps this is as good as can be expected with the use of this simple theory. However, the large three-body collision effect on the vibrational relaxation of this system complicates the interpretation of the data and makes the significance of the comparison dubious.

Huber and Kantrowitz (25) have measured the effect of water on the relaxation time of nitrogen by the impact tube method. A portion of their data is reproduced in Table 9.

Table 9

Experimental Data On Relaxation Times of N_2 - H_2O Mixtures Due to Huber and Kantrowitz (25)

% H_2O	T $^{\circ}K$	τ (Sec. - atm.) x 10^3
0.05	556	5.9
0.05	680	2.9
0.05	686	2.7
0.05	694	3.4
0.05	761	2.6
0.66	561	0.62
0.97	712	0.39
1.33	560	0.37
1.41	709	0.28
1.45	733	0.26
1.99	575	0.23
2.97	708	0.14
3.5	413	0.12

They state that the driest nitrogen used in their experiments had a water content of about 0.05%. On the basis of the effect of H_2O on O_2 it is expected that even this small amount of water vapor would reduce the nitrogen relaxation time considerably.

Lukasik and Young (28) have measured the relaxation time of nitrogen in the temperature range 778° - 1186°K. Their nitrogen was reported to contain less than 0.005% water vapor. The data of Lukasik and Young are in good agreement with the extropolated results of Blackman determined by the interferometer method at temperatures of 3500 - 5600°K. In Table 10 a comparison is presented between the theoretically derived non-resonant probabilities for nitrogen and the values obtained from the combined data of Blackman and Lukasik extropolated into the temperature range of the Huber - Kantrowitz experiments. The agreement is within an order of magnitude.

Table 10

Comparison of Non-Resonant Probabilities for Nitrogen

	$P^{10}_{(N_2)}$	$P^{10}_{(N_2)}$
T	Theoretical	Experimental (28)
°K	x 10^9	x 10^9
400	0.046	0.50
500	0.25	2.5
600	1.0	7.1
700	3.2	25
800	8.5	50

Using the experimental non-resonant probabilities from Table 10 to estimate the relaxation times of pure nitrogen, the probabilities of the near-resonant process for N_2 - H_2O collisions have been calculated from the Huber - Kantrowitz data. The results are plotted in Figure 8 as a function of temperature. The solid curve represents the theoretical

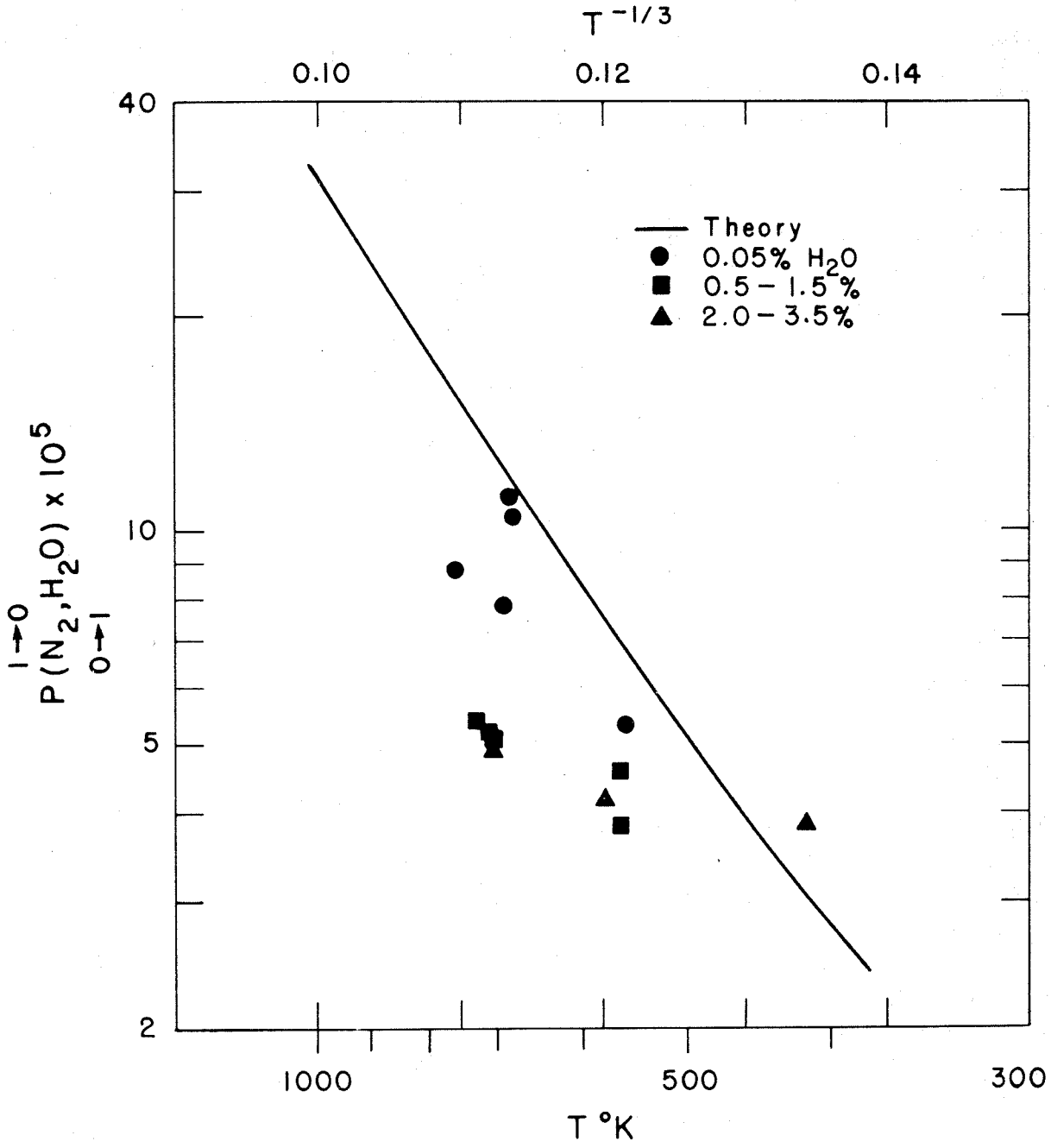

Fig.8 —Comparison of near-resonant probability for N_2-H_2O system.

near-resonant probability calculated from equations 46 and 47. The Lennard - Jones parameters used in the theoretical calculation are listed in Table 8. The agreement between the theoretical curve and the experimental values is seen to be within a factor of two or three for a reasonably wide range of temperatures and concentrations of water vapor.

In Part I of this thesis, Table 3, the effect of water vapor on the vibrational relaxation of pure carbon monoxide is given for two experimental conditions. The near-resonant probabilities calculated from this data are: $T = 1400^{\circ}K$, $\% H_2O = 0.002$, $P(CO, H_2O)^{10}_{01} = 1.8 \times 10^{-2}$; $T = 1430^{\circ}K$, $\% H_2O = 0.3$, $P(CO, H_2O)^{10}_{01} > 1.3 \times 10^{-3}$. The theoretical calculation of the near-resonant probability yields 4.1×10^{-3}. Since carbon monoxide has a very small dipole moment, it was assumed to be non-polar, and σ and ϵ for the CO - H_2O interaction obtained as before with nitrogen and oxygen. These parameters are also given in Table 8.

It is apparent that the experimentally derived probabilities differ by a factor of ten. The value for the higher concentration of water vapor (0.3%) is considered more reliable. At the lower concentration (0.002%) small amounts of other polyatomic impurities may also be affecting the relaxation of the gas. The value at the higher concentration is only a lower limit, since the measured relaxation time is close to the response time of the detector and may be smaller.

The results of this discussion of the effect of water vapor upon the vibrational relaxation of oxygen, nitrogen, and carbon monoxide illustrate that the resonant energy exchange process may be useful in the interpretation of the impurity effect on the relaxation of simple gases. It is

not suggested that the resonant mechanism can at present explain the effects of all impurity gases nor even of all the known examples of water. In the CO_2 - H_2O system at room temperature, for example, the experimental evidence indicates that energy is exchanged between a CO_2 and H_2O molecule every tenth collision or less. The calculations presented for the systems O_2 - H_2O, N_2 - H_2O, and CO - H_2O indicate that the S-S-H theory of vibrational energy exchange is not successful in predicting such a probable process even at exact resonance.

Summary

The results of this investigation emphasize the importance of a resonant or near-resonant energy exchange mechanism on the vibrational relaxation of a mixture of two gases. The resonant mechanism is shown to have a large effect on the equilibration of the vibrational energy of the mixture when: (a) the two components have widely different relaxation times in the pure state, and (b) the resonant exchange of energy is much more probable than the non-resonant excitation of the slower relaxing gas. Under these conditions a catalytic effect on the relaxation time of the slower component is predicted, and the relaxation of the fast component is decreased to some extent. However, the principal contribution of the resonant process is to provide a path for the rapid vibrational equilibration of a gas with a long, non-resonant relaxation time.

Detailed calculations are presented for mixtures of oxygen and nitrogen illustrating this behavior. There is, as yet, meager experimental evidence to test the validity of these hypothetical calculations. The data of one experiment on oxygen - nitrogen mixtures do not exhibit the predicted effect, although the presence of a smaller resonant process is not contradicted. With the considerable recent interest in high speed flight the high temperature, transient properties of air assume great importance. It is obvious from the present calculations that the incorporation of a near-resonant mechanism into the vibrational relaxation of air is of aerodynamic importance below 5000°K. This would suggest that further experimental work on the nitrogen - oxygen system is needed to determine the magnitude, if any, of the resonant process.

The vibrational relaxation of pure polyatomic gases offers the best available experimental evidence for the existence of a resonant process. Both

sulfur dioxide and methylene chloride show relaxation times which appear to be due to a near-resonant exchange of energy between low lying vibrational modes of these molecules. If the resonant process is accepted, it offers a possible explanation of the large influence of so-called impurity gases on vibrational relaxation times. This point has been illustrated by some calculations on the systems of $N_2 - H_2O$, $O_2 - H_2O$, and $CO - H_2O$.

There are many two component gas systems in which a resonant or near-resonant exchange of vibrational energy is possible. Experiments are particularly needed on systems of relatively simple molecules, since only in these cases will a comparison with present theory be meaningful.

APPENDIX I

Numerical Integration Procedure

To solve the set of two, coupled, non-linear differential equations, 23 and 24, a numerical method of integration was employed. The method is based on the general fourth-order processes due to Kutta (29) as modified by Gill (30) for machine computation.

Consider a single first-order differential equation

$$\frac{dy}{dx} = f(x, y) \tag{A-1}$$

The value of y at some point, X_o, is known, and it is desired to find the value of y at the point $X_o + h$. By substituting the values X_o, Y_o into A-1, the slope of the function can be found and used to approximate the increment in Y, k_o, due to the increment in X, h

$$k_o = h\, f(X_o, Y_o) \tag{A-2}$$

A second approximation to the increment in y, k_1, is obtained by evaluating the slope of y a fraction m of the way along the straight line defined by A-2 or

$$k_1 = h\, f(X_o + m\,h,\ Y_o + m\,k_o) \tag{A-3}$$

Third and fourth approximations are obtained in like manner

$$k_2 = h\, f(X_o + n h,\ Y_o + [n - r]\,k_o + r k_1) \tag{A-4}$$

$$k_3 = h f(X_o + p h,\ Y_o + [p - S - t]\,k_o + S k_1 + t k_2) \tag{A-5}$$

the final solution is obtained by suitably combining k_o, k_1, k_2, and k_3

$$\Delta y = a k_o + b k_1 + c k_2 + d k_3 \qquad \text{(A-6)}$$

where

$$a + b + c + d = 1 \qquad \text{(A-7)}$$

To determine the conditions on the coefficients m, n, ...t and a...d, one expands $y = y(X_o + h) - y(X_o)$ and A-6 in power series in h and equates coefficients of like powers of h. If this program is carried out through powers of h^4 then the following set of relations is obtained.

$$\begin{aligned}
&a + b + c + d = 1 \quad , \quad b m^3 + c n^3 + d p^3 = 1/4 \\
&b m + c n + d p = 1/2 \quad , \quad c m n r + d(nt + ms)p = 1/8 \\
&b m^2 + c n^2 + d p^2 = 1/3 \quad , \quad c m^2 r + d(n^2 t + m^2 s) = 1/12 \\
&c m r + d(nt + ms) = 1/6 \quad , \quad d m r t = 1/24
\end{aligned} \qquad \text{(A-8)}$$

This is a set of eight equations in ten unknowns, and, therefore, there are two degrees of freedom. Kutta set p = 1, retaining one degree of freedom, and solved A-8 for several special cases with fairly simple forms. One particularly simple form is the well-known Runge - Kutta or Kutta's Simpson's rule in which the coefficients become:

$$\begin{aligned}
&m = \tfrac{1}{2} \quad , \quad r = \tfrac{1}{2} \\
&n = \tfrac{1}{2} \quad , \quad s = 0 \\
&p = 1 \quad , \quad t = 1 \\
&a = 1/6,\ b = 1/3,\ c = 1/3,\ d = 1/6
\end{aligned} \qquad \text{(A-9)}$$

The extension of this general approach to a set of simultaneous first-order equations is straightforward. For a set of n equations of the type

$$\frac{dy_i}{dx} = f_i(x, y_1, y_2, \ldots y_n), \quad (i = 1, \ldots n) \qquad \text{(A-10)}$$

the relations A-2 to A-7 become

$$\begin{aligned} k_{i0} &= h f_i(Y_0, Y_1, \dots) \\ k_{i1} &= h f_i(Y_0 + m k_{00}, Y_1 + m k_{10}, \dots) \\ k_{i2} &= h f_i(Y_0 + [n-r]k_{00} + r k_{10}, \dots) \qquad (i = 0, 1 \dots n) \\ k_{i3} &= h f_i(Y_0 + [p-s-t]k_{00} + s k_{01} + t k_{02}, \dots) \\ \Delta y_i &= a k_{i0} + b k_{i1} + c k_{i2} + d k_{i3} \end{aligned} \tag{A-11}$$

where, for convenience, the transformation $x = y_0$ has been used in A-10 to make all the variables dependent.

If the sequence of operations indicated in A-11 is carried out, it is evident that the calculation of a maximum number of four independent quantities occurs in the third state. These quantities are

$$\begin{aligned} &Y_i + [n-r]k_{i0} + r k_{i1} \\ &Y_i + [p-s-t]k_{i0} + s k_{i1} \\ &Y_i + a k_{i0} + b k_{i1} \\ &k_{i2} \end{aligned} \tag{A-12}$$

In a machine calculation a minimum number of four storage registers per equation would be needed. Gill has reduced this number to three by making the quantities A-12 linearly dependent by means of the relation

$$\begin{pmatrix} 1 & n-r & r \\ 1 & p-s-t & s \\ 1 & a & b \end{pmatrix} = 1 \tag{A-13}$$

This condition is not incompatible with equation A-8 and, with the usual condition $p = 1$, leads to a simple solution in which the coefficients become

$$\begin{aligned} m &= 1/2 & r &= 1 - \sqrt{1/2} \\ n &= 1/2 & s &= -\sqrt{1/2} \\ p &= 1 & t &= 1 + \sqrt{1/2} \end{aligned} \tag{A-14}$$

$$a = 1/6\,, \quad b = 1/3(1-\sqrt{1/2})\,, \quad c = 1/3(1+\sqrt{1/2})\,, \quad d = 1/6$$

with these values the final form of the method is

$$
\begin{aligned}
k_{i0} &= h f_i(Y_{00}, Y_{10}, Y_{20}, \ldots Y_{n0}) \\
Y_{i1} &= Y_{i0} + \tfrac{1}{2} k_{i0} \\
q_{i1} &= k_{i0} \\
\\
k_{i1} &= h f_i(Y_{01}, Y_{11}, Y_{21}, \ldots Y_{n1}) \\
Y_{i2} &= Y_{i1} + [1 - \sqrt{1/2}](k_{i1} - q_{i1}) \\
q_{i2} &= [2 - \sqrt{2}]\, k_{i1} + [-2 + 3\sqrt{1/2}]\, q_{i1} \\
\\
k_{i2} &= h f_i(Y_{02}, Y_{12}, Y_{22}, \ldots Y_{n2}) \\
Y_{i3} &= Y_{i2} + [1 + \sqrt{1/2}](k_{12} - q_{12}) \\
q_{i3} &= [2 + \sqrt{2}]\, k_{i2} + [-2 - 3\sqrt{1/2}]\, q_{i2} \\
\\
k_{i3} &= h f_i(Y_{03}, Y_{13}, Y_{23}, \ldots Y_{n3}) \\
Y_{i4} &= Y_{i3} + \tfrac{1}{6} k_{i3} - \tfrac{1}{3} q_{i3}
\end{aligned}
\qquad \text{(A-15)}
$$

A "dummy" variable, q, has been introduced in A-15 so that at each stage the most recently calculated k's, y's and q's can be stored over the previous values which are now no longer needed. The maximum number of three storage registers per equation is evident. The error of the method is of the order of h^5. In common with the Runge - Kutta procedure this method also employs only values of the independent variable at the ends and middle of the interval and is thereby convenient for tabulated functions.

A 282 word program utilizing this method was written for use on the Datatron Computer, Model 205. The program was designed to handle a maximum of 19 equations of the type A-10 and employed floating point operations. Gill (30) has modified the basic method to correct for round-off error inherent in fixed point operation. The time for calculation of one interval for the particular equations of this problem was approximately one second, and a complete integration of the equations took between 5 to 10 minutes.

APPENDIX II

Numerical Data of Vibrational Relaxation in Oxygen-Nitrogen Mixture

Table 11

1000°K

Pure O_2		Pure N_2		1% O_2 - 99% N_2		
t μsec	$E_A/\bar{E}_A$	t μsec x 10^{-2}	$E_B/\bar{E}_B$	t μsec	$E_A/\bar{E}_A$	$E_B/\bar{E}_B$
2.3	0.05	5.4	0.08	2.3	0.05	0.0003
5.1	0.12	9.5	0.13	5.1	0.11	0.0008
9.1	0.20	13.5	0.18	9.1	0.19	0.002
12.3	0.26	19.7	0.25	12.3	0.24	0.002
15.5	0.31	27.9	0.34	18.7	0.33	0.004
18.7	0.36	33.5	0.39	25.1	0.40	0.006
25.1	0.45	40.7	0.45	31.5	0.45	0.008
31.5	0.53	47.9	0.51	44.3	0.53	0.01
37.9	0.60	64.8	0.62	63.5	0.60	0.02
44.3	0.66	75.0	0.67	101.9	0.65	0.03
57.1	0.75	93.95	0.75	242.7	0.68	0.09
76.3	0.84	119.5	0.83	421.9	0.71	0.15
101.9	0.91	150.3	0.89	575.5	0.72	0.20
153.1	0.97	199.4	0.95	780.3	0.74	0.27
537.1	1.00	215.8	0.96	985.1	0.77	0.32
				1190	0.78	0.37
				1446	0.80	0.44
				1753	0.83	0.50
				2060	0.85	0.56
				2419	0.87	0.62
				3187	0.91	0.72

Table 11 - Continued

3187	0.92	0.78
4415	0.94	0.83
5286	0.96	0.88
6668	0.98	0.93

10% O_2 - 90% N_2			20% O_2 - 80% N_2			50% O_2 - 50% N_2		
t μsec.	$E_A/\bar{E}_A$	$E_B/\bar{E}_B$	t μsec.	$E_A/\bar{E}_A$	$E_B/\bar{E}_B$	t μsec.	$E_A/\bar{E}_A$	$E_B/\bar{E}_B$
2.4	0.06	0.001	2.3	0.05	0.001	2.3	0.05	0.002
5.2	0.11	0.002	5.1	0.11	0.003	5.1	0.11	0.006
9.2	0.19	0.005	9.1	0.19	0.008	9.1	0.19	0.02
12.4	0.24	0.008	12.3	0.24	0.01	12.3	0.25	0.03
18.8	0.33	0.02	18.7	0.33	0.03	15.5	0.30	0.05
25.2	0.40	0.03	25.1	0.41	0.05	21.9	0.39	0.08
31.6	0.46	0.04	31.5	0.47	0.07	28.3	0.46	0.12
44.4	0.55	0.06	37.9	0.52	0.09	37.9	0.56	0.19
57.2	0.60	0.09	50.7	0.60	0.13	50.7	0.65	0.29
76.4	0.66	0.13	63.5	0.65	0.18	63.5	0.72	0.38
102.0	0.70	0.19	89.1	0.72	0.28	76.3	0.77	0.46
127.6	0.73	0.24	114.7	0.77	0.37	89.1	0.81	0.54
153.2	0.75	0.29	153.1	0.81	0.48	101.9	0.84	0.60
191.6	0.77	0.36	178.7	0.84	0.55	114.7	0.87	0.66
242.8	0.80	0.44	204.3	0.86	0.60	127.5	0.89	0.71
294.0	0.83	0.51	229.9	0.88	0.65	153.1	0.92	0.79
370.8	0.86	0.61	306.7	0.92	0.77	178.7	0.94	0.85
422.0	0.88	0.65	357.9	0.94	0.82	229.9	0.97	0.93
524.4	0.91	0.74	460.3	0.96	0.90	306.7	0.99	0.98
678.0	0.94	0.83	613.9	0.98	0.95			
882.8	0.97	0.90						
1139	0.98	0.95						

Table 12

2000°K

Pure O_2		Pure N_2		1% O_2 - 99% N_2		
t μsec	$E_A/\bar{E}_A$	t μsec	$E_B/\bar{E}_B$	t μsec	$E_A/\bar{E}_A$	$E_B/\bar{E}_B$
0.13	0.05	5.1	0.04	0.13	0.05	0.001
0.27	0.11	16.6	0.13	0.27	0.11	0.002
0.51	0.19	24.3	0.18	0.51	0.19	0.004
0.67	0.25	37.1	0.26	0.91	0.30	0.008
0.91	0.32	47.3	0.32	1.2	0.37	0.01
1.2	0.40	57.5	0.37	1.5	0.44	0.01
1.5	0.48	78.0	0.47	2.2	0.53	0.02
2.2	0.60	98.5	0.55	2.8	0.60	0.03
2.8	0.70	113.9	0.60	3.8	0.66	0.04
3.8	0.80	134.8	0.66	6.4	0.74	0.06
5.1	0.88	154.8	0.72	14.0	0.78	0.13
8.9	0.98	190.7	0.79	24.3	0.80	0.22
16.6	1.00	231.6	0.85	37.1	0.82	0.32
		282.8	0.90	47.3	0.84	0.39
		375.0	0.95	57.6	0.85	0.45
				67.8	0.87	0.50
				78.0	0.88	0.55
				98.5	0.90	0.64
				113.9	0.92	0.69
				136.9	0.94	0.76
				167.6	0.95	0.83
				208.6	0.97	0.89
				270.0	0.98	0.94
				285.4	0.99	0.95

Table 12 - Continued

10% O_2 - 90% N_2			20% O_2 - 80% N_2			50% O_2 - 50% N_2		
t μsec	$E_A/\bar{E}_A$	$E_B/\bar{E}_B$	t μsec	$E_A/\bar{E}_A$	$E_B/\bar{E}_B$	t μsec	$E_A/\bar{E}_A$	$E_B/\bar{E}_B$
0.13	0.05	0.001	0.16	0.06	0.002	0.13	0.05	0.002
0.27	0.11	0.003	0.32	0.12	0.004	0.27	0.11	0.004
0.51	0.19	0.006	0.60	0.22	0.009	0.51	0.19	0.01
0.91	0.30	0.01	1.1	0.35	0.02	0.67	0.24	0.02
1.2	0.38	0.02	1.4	0.42	0.03	0.91	0.31	0.03
1.5	0.44	0.02	1.9	0.50	0.05	1.2	0.39	0.05
2.2	0.54	0.04	2.5	0.59	0.07	1.5	0.46	0.07
2.8	0.61	0.05	3.2	0.65	0.10	2.2	0.57	0.11
3.8	0.68	0.08	4.4	0.73	0.15	2.8	0.65	0.16
5.1	0.73	0.11	5.7	0.78	0.20	3.8	0.74	0.24
8.9	0.80	0.21	7.6	0.82	0.28	5.1	0.81	0.35
11.4	0.82	0.27	10.2	0.85	0.37	6.4	0.86	0.44
14.0	0.83	0.33	12.8	0.87	0.46	8.9	0.91	0.60
16.6	0.84	0.38	15.3	0.89	0.53	11.5	0.94	0.71
24.3	0.88	0.51	17.9	0.90	0.59	15.3	0.96	0.83
29.4	0.89	0.58	21.7	0.92	0.67	20.4	0.98	0.91
37.1	0.92	0.67	26.8	0.94	0.75	25.6	0.99	0.96
47.3	0.94	0.76	32.0	0.95	0.81			
57.6	0.96	0.83	42.2	0.97	0.89			
78.0	0.98	0.91	57.6	0.99	0.96			
98.5	0.99	0.96						

Table 13

3000°K

Pure O_2		Pure N_2		1% O_2 - 99% N_2		
t μsec	$E_A/\bar{E}_A$	t μsec	$E_B/\bar{E}_B$	t μsec	$E_A/\bar{E}_A$	$E_B/\bar{E}_B$
0.035	0.05	0.89	0.05	0.036	0.05	0.002
0.075	0.11	2.3	0.12	0.076	0.11	0.004
0.12	0.18	3.6	0.19	0.12	0.17	0.007
0.19	0.26	5.1	0.25	0.19	0.25	0.01
0.25	0.33	6.7	0.32	0.25	0.31	0.01
0.31	0.39	8.7	0.39	0.32	0.37	0.02
0.38	0.45	10.7	0.46	0.38	0.42	0.02
0.44	0.50	12.8	0.52	0.51	0.51	0.03
0.57	0.59	14.8	0.57	0.64	0.58	0.04
0.76	0.70	18.9	0.66	0.76	0.63	0.04
0.89	0.76	23.0	0.73	1.0	0.70	0.06
1.1	0.84	27.1	0.79	1.5	0.77	0.09
1.5	0.91	35.3	0.87	2.6	0.82	0.15
2.3	0.97	51.7	0.95	3.6	0.83	0.20
3.6	1.00	59.9	0.97	4.9	0.85	0.26
				6.4	0.86	0.33
				8.4	0.88	0.41
				10.5	0.89	0.48
				13.6	0.91	0.58
				15.6	0.93	0.63
				22.8	0.95	0.76
				26.9	0.96	0.82
				32.0	0.97	0.87
				40.2	0.99	0.92

Table 13 - Continued

						47.4	0.99	0.95
10% O_2 - 90% N_2			20% O_2 - 80% N_2			50% O_2 - 50% N_2		
t μsec	$E_A/\bar{E}_A$	$E_B/\bar{E}_B$	t μsec	$E_A/\bar{E}_A$	$E_B/\bar{E}_B$	t μsec	$E_A/\bar{E}_A$	$E_B/\bar{E}_B$
0.035	0.05	0.002	0.035	0.05	0.002	0.036	0.06	0.002
0.075	0.11	0.005	0.075	0.11	0.005	0.076	0.11	0.006
0.12	0.17	0.008	0.12	0.17	0.009	0.12	0.18	0.01
0.19	0.25	0.01	0.19	0.25	0.01	0.19	0.25	0.02
0.25	0.31	0.02	0.25	0.32	0.02	0.25	0.32	0.03
0.31	0.37	0.02	0.31	0.38	0.03	0.32	0.38	0.04
0.38	0.43	0.03	0.38	0.43	0.03	0.38	0.44	0.05
0.51	0.51	0.04	0.51	0.52	0.05	0.51	0.53	0.08
0.64	0.58	0.05	0.64	0.59	0.07	0.64	0.61	0.11
0.76	0.63	0.06	0.76	0.64	0.08	0.76	0.67	0.14
1.0	0.71	0.09	1.0	0.72	0.12	1.0	0.75	0.21
1.5	0.79	0.14	1.3	0.77	0.16	1.3	0.81	0.28
2.0	0.82	0.19	1.8	0.83	0.23	1.5	0.85	0.34
2.8	0.85	0.26	2.3	0.86	0.30	1.8	0.88	0.40
3.6	0.86	0.33	2.8	0.88	0.36	2.0	0.90	0.45
4.3	0.88	0.39	3.3	0.89	0.42	2.3	0.91	0.50
5.4	0.89	0.46	3.8	0.90	0.47	2.8	0.94	0.59
6.4	0.90	0.52	4.9	0.92	0.56	3.3	0.95	0.67
7.4	0.91	0.58	5.9	0.93	0.64	3.8	0.96	0.73
9.5	0.93	0.67	7.4	0.95	0.73	4.9	0.97	0.82
11.5	0.95	0.74	9.5	0.96	0.81	5.9	0.98	0.88
13.6	0.96	0.80	11.5	0.98	0.87	7.4	0.99	0.93
16.6	0.97	0.86	15.6	0.99	0.94	8.4	0.99	0.96
20.7	0.98	0.92	17.7	1.00	0.96			
26.9	0.99	0.96						

Table 14

4000°K

Pure O_2		Pure N_2		1% O_2 - 99% N_2		
t μsec x 10	$E_A/\bar{E}_A$	t μsec x 10	$E_B/\bar{E}_B$	t μsec x 10	$E_A/\bar{E}_A$	$E_B/\bar{E}_B$
0.14	0.05	2.3	0.05	0.14	0.05	0.003
0.28	0.10	6.1	0.12	0.28	0.10	0.006
0.44	0.16	8.2	0.15	0.44	0.15	0.009
0.64	0.22	12.3	0.22	0.64	0.21	0.01
0.89	0.29	16.4	0.28	0.89	0.28	0.02
1.1	0.36	20.5	0.34	1.1	0.34	0.02
1.5	0.45	24.6	0.39	1.5	0.42	0.03
1.8	0.50	30.7	0.47	2.0	0.51	0.04
2.3	0.59	38.9	0.55	2.6	0.58	0.05
3.1	0.69	47.1	0.62	3.1	0.63	0.06
3.6	0.75	59.4	0.70	4.1	0.71	0.08
4.6	0.83	75.8	0.79	6.1	0.79	0.12
6.1	0.91	92.2	0.85	9.2	0.84	0.18
8.2	0.96	124.9	0.92	12.3	0.85	0.23
12.3	0.99	141.3	0.94	17.4	0.87	0.31
16.4	1.00	157.7	0.96	21.5	0.88	0.37
				25.6	0.89	0.42
				33.8	0.91	0.52
				42.0	0.92	0.59
				54.3	0.94	0.69
				62.5	0.95	0.74
				78.8	0.98	0.82
				95.2	0.98	0.87

Table 14 - Continued

						119.8	0.99	0.92
						144.4	0.99	0.95
10% O_2 - 90% N_2			20% O_2 - 80% N_2			50% O_2 - 50% N_2		
t μsec x 10	$E_A/\bar{E}_A$	$E_B/\bar{E}_B$	t μsec x 10	$E_A/\bar{E}_A$	$E_B/\bar{E}_B$	t μsec x 10	$E_A/\bar{E}_A$	$E_B/\bar{E}_B$
0.14	0.05	0.003	0.14	0.05	0.003	0.14	0.05	0.003
0.28	0.10	0.006	0.28	0.10	0.006	0.28	0.10	0.007
0.44	0.15	0.009	0.44	0.16	0.01	0.44	0.16	0.01
0.64	0.21	0.01	0.64	0.21	0.01	0.64	0.22	0.02
0.89	0.28	0.02	0.89	0.28	0.02	0.89	0.29	0.03
1.1	0.34	0.03	1.1	0.35	0.03	1.1	0.35	0.04
1.5	0.42	0.04	1.5	0.43	0.04	1.5	0.43	0.06
2.0	0.51	0.05	2.0	0.52	0.06	2.0	0.53	0.08
2.6	0.58	0.06	2.6	0.59	0.07	2.6	0.60	0.11
3.1	0.64	0.08	3.1	0.64	0.09	3.1	0.66	0.14
4.1	0.72	0.10	4.1	0.73	0.13	4.1	0.75	0.20
5.1	0.77	0.13	5.1	0.78	0.16	5.1	0.81	0.26
7.2	0.82	0.19	7.2	0.84	0.24	6.1	0.85	0.31
9.2	0.85	0.24	9.2	0.87	0.30	7.2	0.88	0.37
12.3	0.87	0.31	11.3	0.89	0.36	8.2	0.90	0.42
15.4	0.89	0.38	13.3	0.90	0.42	10.2	0.93	0.51
19.5	0.90	0.45	15.4	0.91	0.47	12.3	0.94	0.59
23.5	0.91	0.52	19.5	0.92	0.56	14.3	0.96	0.66
29.7	0.93	0.61	23.5	0.94	0.63	16.4	0.96	0.71
37.9	0.94	0.70	29.7	0.95	0.72	20.5	0.97	0.80
46.1	0.96	0.77	37.9	0.97	0.81	24.6	0.98	0.86

Table 14 - Continued

54.3	0.97	0.82	46.1	0.98	0.87	32.8	0.99	0.93
95.2	0.99	0.95	62.5	0.99	0.93	41.0	1.00	0.96
			70.7	0.99	0.95			

Table 15

5000°K

Pure O_2		Pure N_2		1% O_2 - 99% N_2		
t μsec x 10	$E_A/\bar{E}_A$	t μsec x 10	$E_B/\bar{E}_B$	t μsec x 10	$E_A/\bar{E}_A$	$E_B/\bar{E}_B$
0.09	0.05	1.2	0.05	0.10	0.06	0.005
0.20	0.11	2.5	0.10	0.20	0.11	0.009
0.31	0.16	2.9	0.12	0.36	0.18	0.02
0.46	0.23	3.7	0.15	0.51	0.25	0.02
0.61	0.30	4.9	0.20	0.72	0.33	0.03
0.82	0.38	6.6	0.26	0.92	0.39	0.04
1.0	0.45	8.2	0.31	1.2	0.48	0.05
1.2	0.51	10.6	0.38	1.6	0.56	0.07
1.4	0.56	13.9	0.47	2.0	0.63	0.09
1.8	0.66	17.2	0.54	2.5	0.68	0.11
2.5	0.76	20.5	0.60	3.3	0.75	0.14
2.9	0.81	23.8	0.65	4.9	0.82	0.20
3.7	0.88	30.3	0.74	6.6	0.84	0.26
4.9	0.94	36.9	0.81	8.2	0.86	0.32
6.6	0.98	50.0	0.89	9.8	0.87	0.37
8.2	0.99	69.6	0.96	12.3	0.89	0.44
				15.6	0.90	0.52
				18.8	0.92	0.58
				23.8	0.93	0.67
				30.3	0.95	0.76
				36.9	0.96	0.82
				46.7	0.98	0.89
				59.8	0.99	0.94
				66.4	0.99	0.96

Table 15 - Continued

10% O_2 - 90% N_2			20% O_2 - 80% N_2			50% O_2 - 50% N_2		
t μsec x 10	$E_A/\bar{E}_A$	$E_B/\bar{E}_B$	t μsec x 10	$E_A/\bar{E}_A$	$E_B/\bar{E}_B$	t μsec x 10	$E_A/\bar{E}_A$	$E_B/\bar{E}_B$
0.10	0.06	0.005	0.10	0.06	0.005	0.09	0.05	0.004
0.20	0.11	0.009	0.20	0.11	0.01	0.20	0.11	0.01
0.36	0.18	0.02	0.36	0.18	0.02	0.31	0.16	0.02
0.51	0.25	0.02	0.51	0.25	0.03	0.46	0.23	0.03
0.72	0.33	0.03	0.72	0.33	0.04	0.61	0.29	0.04
0.92	0.39	0.04	0.92	0.40	0.05	0.82	0.37	0.05
1.2	0.48	0.06	1.2	0.48	0.07	1.0	0.43	0.07
1.6	0.57	0.08	1.6	0.57	0.09	1.2	0.49	0.09
2.0	0.64	0.10	2.0	0.64	0.12	1.4	0.54	0.10
2.5	0.69	0.12	2.5	0.70	0.14	1.8	0.63	0.14
3.3	0.76	0.17	3.3	0.77	0.19	2.5	0.72	0.20
4.9	0.83	0.25	4.9	0.85	0.29	3.3	0.80	0.28
6.6	0.86	0.32	6.6	0.88	0.38	4.1	0.85	0.35
8.2	0.88	0.39	8.2	0.90	0.46	4.9	0.89	0.42
9.8	0.89	0.45	9.8	0.92	0.52	5.7	0.91	0.48
11.5	0.90	0.50	11.5	0.93	0.58	6.6	0.92	0.53
13.9	0.92	0.57	13.9	0.94	0.66	7.4	0.94	0.59
17.2	0.93	0.65	17.2	0.95	0.74	9.0	0.95	0.67
20.5	0.94	0.72	20.5	0.97	0.80	10.6	0.96	0.74
23.8	0.95	0.77	27.0	0.98	0.88	12.3	0.97	0.79
30.3	0.97	0.85	36.9	0.99	0.95	15.6	0.98	0.87
36.9	0.98	0.90	43.4	1.00	0.97	20.5	0.99	0.94
50.0	0.99	0.96				23.8	0.99	0.96

Table 16

8000°K

Pure O_2		Pure N_2		1% O_2 - 99% N_2		
t μsec x 10^2	$E_A/\bar{E}_A$	t μsec x 10^2	$E_B/\bar{E}_B$	t μsec	$E_A/\bar{E}_A$	$E_B/\bar{E}_B$
0.32	0.05	3.1	0.05	0.31	0.05	0.005
0.76	0.12	7.2	0.12	0.76	0.12	0.01
1.1	0.18	9.2	0.15	1.1	0.17	0.02
1.5	0.23	12.3	0.19	1.8	0.25	0.03
2.0	0.29	16.4	0.24	2.3	0.31	0.04
2.6	0.35	20.5	0.30	3.1	0.39	0.05
3.1	0.40	28.7	0.39	4.1	0.47	0.07
4.1	0.50	36.9	0.47	5.1	0.55	0.08
5.1	0.58	45.1	0.54	6.1	0.60	0.10
6.1	0.64	53.2	0.60	8.2	0.69	0.13
7.2	0.70	61.4	0.65	10.2	0.75	0.16
9.2	0.79	77.8	0.74	14.3	0.82	0.22
12.3	0.87	94.2	0.80	18.4	0.86	0.27
16.4	0.94	118.8	0.87	24.6	0.89	0.35
20.5	0.97	151.5	0.93	32.8	0.91	0.43
28.7	0.99	184.3	0.96	41.0	0.92	0.51
				49.1	0.93	0.58
				57.3	0.94	0.63
				73.7	0.96	0.72
				98.3	0.97	0.82
				131.1	0.99	0.90
				172.0	0.99	0.94
				180.2	1.00	0.95

Table 16 - Continued

10% O_2 - 90% N_2			20% O_2 - 80% N_2			50% O_2 - 50% N_2		
t usec x 10^2	$E_A/\bar{E}_A$	$E_B/\bar{E}_B$	t μsec x 10^2	$E_A/\bar{E}_A$	$E_B/\bar{E}_B$	t μsec x 10^2	$E_A/\bar{E}_A$	$E_B/\bar{E}_B$
0.31	0.05	0.005	0.31	0.05	0.005	0.32	0.05	0.006
0.76	0.12	0.01	0.76	0.12	0.01	0.76	0.12	0.01
1.1	0.17	0.02	1.1	0.17	0.02	1.1	0.17	0.02
1.8	0.25	0.03	1.5	0.22	0.03	1.5	0.22	0.03
2.3	0.31	0.04	2.0	0.28	0.04	2.0	0.29	0.04
3.1	0.39	0.05	2.6	0.34	0.05	2.6	0.34	0.05
4.1	0.48	0.07	3.1	0.39	0.06	3.1	0.40	0.07
5.1	0.55	0.09	4.1	0.48	0.08	4.1	0.49	0.09
6.1	0.61	0.11	5.1	0.55	0.10	5.1	0.56	0.12
8.2	0.70	0.14	6.1	0.61	0.12	6.1	0.62	0.14
10.2	0.76	0.18	8.2	0.70	0.16	7.2	0.68	0.17
14.3	0.83	0.25	10.2	0.76	0.20	9.2	0.76	0.23
18.4	0.87	0.31	14.3	0.84	0.27	12.3	0.83	0.30
24.6	0.90	0.39	18.4	0.88	0.35	16.4	0.89	0.40
28.7	0.91	0.44	24.6	0.91	0.44	20.5	0.93	0.49
36.9	0.92	0.53	28.7	0.92	0.49	24.6	0.94	0.56
49.1	0.94	0.64	32.8	0.93	0.54	28.7	0.96	0.63
57.3	0.95	0.70	41.0	0.94	0.63	32.8	0.96	0.68
73.7	0.97	0.79	49.1	0.96	0.70	41.0	0.97	0.77
98.3	0.98	0.87	57.3	0.96	0.76	49.1	0.98	0.83
131.1	0.99	0.94	73.7	0.98	0.84	61.4	0.99	0.90
147.5	0.99	0.95	98.3	0.99	0.91	86.0	1.00	0.96
			131.1	0.99	0.96			

REFERENCES

1. R. N. Schwartz, Z. I. Slawsky, and K. F. Herzfeld, J. Chem. Phys. 20, 1591 (1952).

2. K. Herzfeld, "Thermodynamics and Physics of Matter," Princeton University Press, Princeton, N. J. (1955), Section H, p. 646.

3. F. I. Tanczos, J. Chem. Phys 25, 439 (1956)

4. C. Zener, Phys. Rev. 38, 277 (1931); 37, 556 (1931)

5. L. Landau and E. Teller, Physik. Z. Sowjetunion 1D, 34 (1936); 11, 18 (1937)

6. H. Kallman and F. London, Z. physik. Chem. B2, 207 (1929)

7. O. K. Rice, Phys. Rev. 38, 1943 (1931)

8. J. M. Jackson and N. F. Mott, Proc. Roy. Soc. London A 137, 703 (1932)

9. N. F. Mott and H. S. W. Massey, "The Theory of Atomic Collisions," Oxford University Press, London (1952), Ed. 2, p. 144.

10. J. O. Hirschfelder, C. F. Curtiss, and R. B. Bird, "Molecular Theory of Gases and Liquids," John Wiley and Sons, Inc., New York (1954) p. 1111

11. R. N. Schwartz and K. E. Herzfeld, J. Chem. Phys. 22, 767 (1954)

12. G. Herzberg, "Spectra of Diatomic Molecules," D. Van Nostrand Co., Inc., New York (1950), Ed. 2, pp. 553, 560.

13. J. O. Hirschfelder et. al., op. cit., p. 168.

14. "Selected Values of Chemical Thermodynamic Properties," National Bureau of Standards, Series III (1947 - 1954).

15. F. R. Gilmore, "Equilibrium Composition and Thermodynamic Properties of Air to 24,000°K," Rand Corp. Research Report RM-1543 (24 August 1955)

16. K. S. Pitzer, "Quantum Chemistry," Prentice-Hall Inc., New York (1954), p. 457

17. H. O. Kneser and V. O. Knudsen, Ann. Physik 21, 682 (1934).

18. V. Blackman, J. Fluid Mech. 1, 61 (1956).

19. D. Sette, A. Busala, and J. C. Hubbard, J. Chem. Phys. 23, 787 (1955)

REFERENCES - Continued

20. J. D. Lambert and R. Salter, Proc. Roy. Soc. A, 243, 78 (1957).

21. G. Herzberg, "Infrared and Ramen Spectra of Polyatomic Molecules," D. Van Nostrand Co., Inc., New York (1945), p. 285.

22. P. G. Dickens and J. W. Linnett, Proc. Roy. Soc. A, 243, 84 (1957).

23. B. Windom and S. H. Bauer, J. Chem. Phys. 21, 1670 (1953).

24. G. Herzberg, "Infrared and Ramen Spectra, etc.," p. 281.

25. P. W. Huber and A. Kantrowitz, J. Chem. Phys. 15, 275 (1947).

26. H. and L. Knötzel, Ann. Physik 2, 393 (1948).

27. J. O. Hirschfelder et. al., op. cit., p. 223.

28. S. J. Lukasik and J. E. Young, J. Chem. Phys. 27, 1149 (1957).

29. W. Kutta, Z. Math. Phys. 46, 435 (1901).

30. S. Gill, Proc. Cambridge Phil. Soc. 47, 96 (1951).

PROPOSITIONS

1. The presently accepted experimental value for the vibrational relaxation time of NO (1,2) is many orders of magnitude shorter than is expected by present theory and by comparison with other simple gases. It is proposed that this experiment is being affected by impurities and needs reinvestigation. An experiment is suggested.

2. It is proposed that the vibrational relaxation time of CO be measured in the presence of small amounts of O_2 and N_2 as the resonant impurities. Such an experiment would provide data by which to evaluate the resonant hypothesis discussed in Part II of this thesis.

3. Some previous measurements of the vibrational relaxation time of CO_2 have been interpreted as showing that the bending vibration of the CO_2 molecule relaxes faster than the stretching mode (3,4,5). An experiment is proposed to measure the relaxation of the two modes simultaneously.

4. The radical addition of HBr to propyne has been found to be stereospecific in the liquid phase. However, a kinetic investigation of the gas phase reaction yielded no conclusion because of the rapid isomer equilibration of the product - 1-bromo-1-propene (6). The gas phase experiment is criticized and further experiments proposed.

5. The detailed numerical solution of the three-body collision problem has been used to obtain information on atom recombination and chemical kinetics (7,8). This method is suggested to investigate some theoretical aspects of vibrational relaxation.

6. In Part II of this thesis it was suggested that the bimolecular effect of H_2O on O_2 vibrational relaxation is due to an exact resonant process. An experiment is proposed to test this hypothesis.

7. In recent years the study of the pyrolysis of simple hydrocarbons by shock wave heating has provided information on the mechanism of carbon formation (9,10). Further experiments along this line are proposed.

8. A recently discovered acetylene tricobalt carbonyl complex (11,12) exhibits an IR spectrum that is similar to that of acetylene absorbed on metal surfaces (13). It is proposed that the structure of such complexes may be useful in determining the bonding of acetylene to surface metal atoms.

9. In a shock tube study of the kinetics of the dissociation of O_2 (14) a delay in the onset of thermal dissociation has been observed. Several experiments are proposed to study the mechanism of this dissociation lag.

10. A study of the vibrational relaxation of H_2 is of interest in order to compare with detailed theoretical calculations (15). An experiment is proposed utilizing electric-field induced transitions in the infrared (16).

REFERENCES FOR PROPOSITIONS

1. Robben, F. A., Bull. Amer. Phys. Soc. 3, 320 (1958), in press - J. Chem. Phys.
2. Bauer, H. J., Kneser, H. O., Sittig, E., J. Chem. Phys. 30, 1119 (1959).
3. Eucken, A. and Küchler, L., Physik. Z. 39, 831 (1938).
4. Pielemeier, Saxtan, and Telfair, J. Chem. Phys. 8, 106 (1940).
5. Griffith, W., ONR Report.
6. Skell, P. S. and Allen, R. G., J. Am. Chem. Soc. 80, 5997 (1958).
7. Wall, F. T., Hiller, L. A., and Mazur, J., J. Chem. Phys. 29, 255 (1958).
8. Engleman, R. and Davidson, N., private communications.
9. Greene, E. F., Taylor, R. L., and Patterson, W. L., Jr., J. Phys. Chem. 62, 238 (1958).
10. Bradley, J., private communication.
11. Markby, R., et al., J. Am. Chem. Soc. 80, 6529 (1958).
12. Sly, W. G., J. Am. Chem. Soc., 81, 18 (1959).
13. Eischens, R. P., J. Chem. Ed. 35, 385 (1958).
14. Vaughan, A. and Camac, N., Bull. Amer. Phys. Soc. 4, 290 (1959), also private communications.
15. Salkoff, M. and Bauer, E., J. Chem. Phys. 29, 26 (1958).
16. Terhune, R. W. and Peters, C. W., J. Mol. Spec. 3, 138 (1959).